Investigation of the Invasion Mechanism Mediated by the Outer Membrane Protein PagN of Salmonella Typhimurium

Emilie Barilleau
National Research Institute for Agriculture, Food and Environment
Mégane Védrine
National Research Institute for Agriculture, Food and Environment
Michael Koczerka
National Research Institute for Agriculture, Food and Environment
Julien Burlaud-Gaillard
Centre Hospitalier Universitaire de Tours
Florent Kempf
National Research Institute for Agriculture, Food and Environment
Olivier Grépinet
National Research Institute for Agriculture, Food and Environment
Isabelle Virlogeux-Payant
National Research Institute for Agriculture, Food and Environment
Philippe Velge
National Research Institute for Agriculture, Food and Environment
Agnès Wiedemann (agnes.wiedemann@inrae.fr)
National Research Institute for Agriculture, Food and Environment

Research Article

Keywords: Salmonella, outer membrane protein, PagN, invasion, actin, Zipper-like entry pathway

Posted Date: January 25th, 2021

DOI: https://doi.org/10.21203/rs.3.rs-150127/v1

Investigation of the invasion mechanism mediated by the outer membrane protein PagN of *Salmonella* Typhimurium

Barilleau Emilie[1], Védrine Mégane[1,2], Koczerka Michael[1], Burlaud-Gaillard Julien[3], Kempf Florent[1], Grépinet Olivier[1], Virlogeux-Payant Isabelle[1], Velge Philippe[1] and Wiedemann Agnès[1,4].

1-INRAE, Université de Tours, ISP, F-37380, Nouzilly, France

2-Present address : Service biologie vétérinaire et santé animale, Inovalys, Angers, France

3-Plateforme IBiSA de Microscopie Electronique, Université de Tours et CHRU de Tours, France.

4-Present address : IRSD - Institut de Recherche en Santé Digestive, Université de Toulouse, INSERM, INRAE, ENVT, UPS, Toulouse, France

Corresponding author:

Dr. Agnès Wiedemann, INSERM U1220, Institut de Recherche en Santé Digestive, Bat B, Purpan Hospital, BP 3028, 31024 Toulouse cedex 03, France. Tel : (+33) 5 62 74 61 42.

E-mail : agnes.wiedemann@inrae.fr

Abstract

Background. *Salmonella* can invade host cells via a type three secretion system called T3SS-1 and its outer membrane proteins, PagN and Rck. However, the mechanism of PagN-dependent invasion pathway used by *Salmonella enterica*, subspecies *enterica* serovar Typhimurium remains unclear.

Results. Here, we report that PagN is well conserved and widely distributed among the different species and subspecies of *Salmonella*. We showed that PagN of *S.* Typhimurium was sufficient and necessary to enable non-invasive *E. coli* over-expressing PagN and PagN-coated beads to bind to and invade different non-phagocytic cells. According to the literature, PagN is likely to interact with heparan sulfate proteoglycan (HSPG) as PagN-mediated invasion could be inhibited by heparin treatment in a dose-dependent manner. This report shows that this interaction is not sufficient to allow the internalization mechanism. Investigation of the role of β1 integrin as co-receptor showed that mouse embryo fibroblasts genetically deficient in β1 integrin were less permissive to PagN-mediated internalization. Moreover, PagN-mediated internalization was fully inhibited in glycosylation-deficient pgsA-745 cells treated with anti-β1 integrin antibody, supporting the hypothesis that β1 integrin and HSPG cooperate to induce the PagN-mediated internalization mechanism. In addition, use of specific inhibitors and expression of dominant-negative derivatives demonstrated that tyrosine phosphorylation and class I phosphatidylinositol 3-kinase were crucial to trigger PagN-dependent internalization, as for the Rck internalization mechanism. Finally, scanning electron microscopy with infected cells showed microvillus-like extensions characteristic of Zipper-like structure, engulfing PagN- coated beads and *E. coli* expressing PagN, as observed during Rck-mediated internalization.

Conclusions. Our results supply new comprehensions into T3SS-1-independent invasion mechanisms of *S.* Typhimurium and highly indicate that PagN induces a phosphatidylinositol 3-kinase signaling pathway, leading to a Zipper-like entry mechanism as the *Salmonella* outer membrane protein Rck.

Running title: PagN-mediated invasion

Keywords: *Salmonella,* outer membrane protein, PagN, invasion, actin, Zipper-like entry pathway

Background

Salmonella is a Gram-negative bacterium, belonging to the *Enterobacteriaceae* family. This genus is divided into two species: *S. bongori* and *S. enterica*. The latter consists of six subspecies: *indica*, *diarizonae*, *arizonae*, *salamae*, *houtenae*, and *enterica* [1]. Currently, more than 2,600 *Salmonella* serovars have been identified [2]. Warm-blooded animals are mainly infected by strains belonging to *S. enterica* subsp. *enterica* [3]. Depending on the host and the serotype, *Salmonella* leads to a wide variety of diseases ranging from gastroenteritis to systemic typhoid fever in both animals and humans. *Salmonella* is spread by the fecal-oral route and can be transmitted through contaminated water and food. After *Salmonella* ingestion, the bacteria are found in the intestine, where they are able to adhere to the intestinal epithelium and to induce their own entry into host cells. This allows *Salmonella* colonization of the intestinal tract, which constitutes a crucial step in establishing infection [2]. To invade non-phagocytic cells, *Salmonella* expresses several invasion factors: a type III secretion system (T3SS) known as T3SS-1, and two invasins Rck and PagN [4].

For many pathogenic bacteria, T3SS are essential virulence factors composed of several substructures that organize into one needle-like structure called an injectisome. This apparatus serves as an entrancefor the bacterial secreted effectors to pass through the inner and outer membranes of the bacterium. When *Salmonella* reaches the small intestine, a neutral pH, a low O_2 tension, high osmolarity and a high iron concentration induce SPI-1 expression. In contrast, the presence of cationic peptides or bile suppresses its expression. The T3SS-1 allows the injection of bacterial effector proteins directly into the host cell. This promotes massive actin polymerization and ruffles membrane rearrangements, leading to bacterial internalization. This invasion mechanism is described as a Trigger mechanism. The contribution of the T3SS-1 in *Salmonella* pathogenesis has been demonstrated but depends on the host [5].

The outer membrane protein Rck (resistance to complement killing) is encoded by the *rck* open reading frame localized on the virulence plasmid [6]. The transcription of *S.* Typhimurium *rck* gene is regulated by SdiA, a quorum sensing regulator [7], which is activated by acyl homoserine lactones (AHL) produced by other bacteria [8, 9]. The Rck outer membrane protein of *S.* Enteritidis is able to interact with EGFR (epidermal growth factor receptor) expressed on the host cell surface, allowing bacterial invasion [10, 11]. A 46 amino-acid region (from G114 to V159) has been shown to be necessary and sufficient to induce the *S.* Enteritidis invasion mechanism [10]. Between the Rck proteins of *S.* Enteritidis and *S.* Typhimurium, this region is very well preserved except for one amino acid substitution (His to Arg) at position 125. The invasion mechanism induced by Rck of *S.* Enteritidis requires induction of a cellular transduction pathway, which has been well characterized. This includes phosphorylation of tyrosine proteins, and activation of PI 3-kinase (phosphatidylinositol 3-kinase), leading to actin polymerization and weak membrane rearrangement [10, 12, 13]. This invasion mechanism is described as a Zipper mechanism [10]. Rck of *S*. Typhimurium is able to induce the bacterial invasion mechanism [14]. However, the signaling cascade leading to the bacterial internalization has not been characterized. The involvement of Rck-EGFR interaction in *Salmonella* pathogenesis remains unclear. However, a *S.* Typhimurium infection performedin a mouse model of intestinal persistence (an asymptomatic carrier state model) demonstrated that Rck was important for the fitness of *Salmonella* in the intestine [15].

The outer membrane protein, PagN (*phoP*-activated gene), has also been identified as a *Salmonella* invasin [16, 17]. It was first identified in *S.* Typhimurium using a Tn*phoA* random-insertion screening designed to identify PhopP-activated genes [18]. The *pagN* gene is localized on the specific centisome 7 genomic island and is present in most serotypes that have been tested [19-21]. The transcription of *pagN* is regulated by the two-component transcriptional regulatory PhoP/PhoQ system. In response to an acidified environment, low Mg^{2+} concentration

or the presence of antimicrobial peptides, PhoQ is auto-phosphorylated and transfers its phosphate to the cytoplasmic DNA-binding protein PhoP that induces or represses the transcription of specific *Salmonella* genes [22]. Lambert *et al.* were the first to demonstrate that *pagN* deletion in *S.* Typhimurium led to a reduction in *Salmonella* invasion of enterocytes [16, 21]. However, the PagN-mediated invasion mechanism remains poorly characterized at the cellular level. The only information known is that actin polymerization is required for promoting PagN-induced bacterial invasion [17] and that PagN uses extracellular heparan sulfate proteoglycans (HSPG) to invade cells [17]. Concerning the role of PagN in *Salmonella* pathogenesis, several studies have shown that *in vivo*, a *S.* Typhimurium *pagN* mutant strain (i) induces less pathological signs in the intestine and survives longer compared to its parental strain in streptomycin-treated mice after oral inoculation and (ii) colonizes the spleen of Balb/C mice less than the wild-type strain after intra-peritoneal inoculation[21, 23].

In this study, we first took advantage of the large number of *Salmonella* genomes available in Enterobase to revisit the distribution of PagN among the *Salmonella* genus. We investigated the link between HSPG and the PagN-mediated internalization mechanism and then characterized the signaling pathway induced during the PagN invasion mechanism of *S.* Typhimurium within host cells to compare it to the mechanism triggered during the Rck-mediated invasion pathway.

Results

PagN invasin is widely distributed and well conserved among the different species and subspecies of *Salmonella*

The presence of the *pagN* ORF was previously studied in only a limited number of *Salmonella* strains belonging to the different species, subspecies and serotypes [19-21, 24]. We took advantage of the great number of *Salmonella* genomes available in the extensive

Enterobase database to reconsider the distribution of this gene and to study its allele and protein diversity within the *Salmonella* genus (*S. bongori* and *S. enterica*). Consistent with previous works, *pagN* was found at a very high frequency in all *S. enterica* subspecies as well as in *S. bongori* species. The percentage of strains harbouring the *pagN* gene ranged from 99.069% for subspecies *S. enterica* subsp. *salamae* to 100 % for *S. bongori* and *S. enterica* subspecies *houtenae* and *indica* (Figure 1A). A total of 944 allelic variants of the *pagN* ORF were observed, ranging from 700 to 755 nucleotides in length. The allele designated as No. 1 was found to be the most represented within the *Salmonella* genus in the database (42.02 % of the recorded genomes). Thus, it was chosen as a reference for all sequence comparisons presented in this section. We then analyzed the distribution of *pagN* allelic variants within *S. bongori* and the six subspecies of *Salmonella enterica* (Figure 1A). For *S. bongori*, we measured a haplotype diversity index of 0.923, which is relatively high. We found 28 different alleles of the gene, each of them presenting low frequencies ($f<0.1$) except the allele designated as No. 51 ($f=0.216$). It is interesting to note that only 4 of the 28 allelic variants were shared with the *S. enterica* species. Strains of the non-*enterica* subspecies of *S. enterica* present various haplotype diversity; we found 69, 33, 24, 23 and 5 alleles for *S. enterica* subsp. *salamae*, *S. enterica* subsp. *arizonae, S. enterica* subsp. *diarizonae*, *S. enterica* subsp. *houtenae*, and *S. enterica* subsp. *Indica,* respectively. This allelic richness is not related to the number of genomes available for each subspecies. This could explain the variation in the calculated haplotype diversity indexes. However, independently of this diversity, a predominant allele was found in each subspecies; *S. arizonae* was mainly associated with allele No. 110 ($f=0.417$), *S. diarizonae* with allele No. 3 ($f=0.538$), *S. houtenae* with allele No. 193 ($f=0.613$) and *S. indica* with allele No. 87 ($f=0.640$). It should be noted that these alleles are specific to these subspecies, as none of these predominant alleles were found in another species or subspecies except allele No. 3, which was found in 3 genomes belonging to subspecies *enterica*. Moreover, the other allelic variants of

151 the gene were rarely shared between non-*enterica Salmonella enterica* subspecies, as only
152 alleles No. 63 and No. 91 were found on two of them (subsp. *arizonae* and *houtenae*).
153 Finally, for *S. enterica* subsp. *enterica* we measured a relatively high haplotype diversity
154 index of 0.803. Possibly due to the number of available genomes, this subspecies presents the
155 highest number of variants in our sample: 781 alleles are found for this subspecies in the dataset
156 (Figure 1A) and allele No. 1 is the predominant one (f=0.424). Other alleles always present low
157 frequencies (f<0.1) in that sample. Moreover, among the 781 allelic variants, only 17 of them
158 (2.17 %) are found in genomes belonging to *S. bongori* species and to other subspecies.
159 Genomes carrying these shared allelic variants belong to a panel of 60 serovars, each showing
160 very different levels of specificity for these variants, their frequencies ranging from 0.0001 to
161 1. Amino-acid sequences of the predominant alleles of *S. bongori* and non-*enterica* subspecies
162 of *S. enterica* were compared to the translated sequence of allele No. 1. They all have a very
163 high percentage of identity with our reference allele (ranging from 82.8 % to 95.0 %), thus
164 highlighting a high conservation of the PagN protein in the *Salmonella* genus (data not shown).
165 We next investigated the distribution of *pagN* allelic variants among the 20 most frequently
166 isolated *Salmonella enterica* subsp. *enterica* serovars in humans in Europe in 2017 [25]. It
167 should be noted that genomes of three of these serovars, i.e. serovars Naples, Java and Kottbus,
168 were not available in Enterobase when the genomes were retrieved for our study. This
169 represented 112,662 genomes, in which 268 alleles were identified. Among these allelic
170 variants, 240 were serovar-specific. Given the low distribution of some allelic variants in this
171 dataset, we only considered the allelic variants carried by at least 1 % of the strains in at least
172 one of these 17 serovars for subsequent analysis. This represented a total of 40 alleles of the
173 *pagN* gene (covering 98.53 % of the 112,662 selected genomes). Under this scheme, we
174 observed that 11 out of the 17 serovars were predominantly associated with one allele. For
175 example, allele designated as N°1 was found at very high frequencies in genomes of *S.*

Enteritidis (f=0.988) and of the monophasic variant of *S.* Typhimurium (antigenic formula: 4;[5];12:i:-) (f=0.993) strains, as well as allele No. 10 that was found at similar frequencies in *S.* Infantis genomes (f=0.993). On the other hand, we also observed other serovars associated with a larger range of alleles, such as *S.* Newport, *S.* Virchow or *S.* Bareilly, consequently showing higher haplotype diversity indexes (Figure 1B). The amino acid sequence alignment of these 40 allelic variants showed high identity with allele No. 1, ranging from 98.7 % to 100 % (Figure 1B).

Taken together, these results confirm that *pagN* is widely distributed within the *Salmonella* genus, and demonstrate that the encoded protein is well conserved among species, subspecies and serovars. They also highlight some allelic specificity at the species, subspecies and serovar levels. This high conservation of PagN suggests an ubiquitous role of this protein, independent of the strain serovar-specificity, and of the pathogenic potential of the strains toward their hosts, although we cannot exclude that some substitutions could be responsible for these phenotypes.

PagN-mediated invasion mechanism depends on the host cell line.

PagN of *S.* Typhimurium has previously been shown to mediate both adhesion to and invasion of CHO cells [16]. Prior to characterizing the invasion mechanism mediated by PagN, we first decided to confirm these results. PagN of *S.* Typhimurium was chosen and a non-invasive *E. coli* HB101 strain harboring either pSUP202 (*HB101-psup*) or pSUP202-PagN (*HB101-pagN*) was used. The percentage of total cell-associated and internalized bacteria was determined using standard adhesion and invasion assays. As shown in Figure 2, we observed that the percentage of total cell-associated and internalized *HB101-pagN* strain was increased 2- and 400- fold, respectively compared to the control strain (*HB101-psup*). Our results confirm that PagN is able to induce bacterial adhesion to and invasion of epithelial cells.

Lambert and Smith showed that PagN utilizes HSPG to invade mammalian cells [17]. HSPG are membrane-anchored proteins with covalently attached glycosaminoglycan side-chains consisting of heparan sulfate (HS) [26]. In order to characterize better the role of HSPG in PagN-mediated invasion, we first determined the expression of HS on the cell surface of different cell lines by flow cytometry using a specific monoclonal anti-HS antibody. The different cell lines chosen were: (i) Caco2 cells, which are mainly used to study the intestinal invasion of *Salmonella* [27]; (ii) HT29 and CHO cell lines as they were previously used to study PagN-mediated invasion mechanism [16, 21]; (iii) proteoglycan-deficient CHO cell line (pgsA745 cells) as a control. The mean percentage of HS positive (HS+) cells showed that HS were detectable on the surface of each cell line but at different levels. As shown in Figure 3A, the mean percentage of HS+ cells is similar in CHO and Caco2 cells, while it is significantly lower in pgsA745 cells and higher in HT29 cells. Next, the ability of *HB101-pagN* to invade these different cell lines was measured. As expected, we observed that the mean percentage of internalized *HB101-pagN* was 1000-fold lower in pgsA745 than CHO cells, confirming the results of Lambert *et al* [17]. Surprisingly, the percentage of internalized bacteria was identical in Caco2 and pgsA745 cells and 10000-fold lower in HT29 cells than in pgsA745 cells (Figure 3B). These results demonstrated that the invasion ability of an *E. coli* strain expressing PagN is not related to the HS exposed on the host cell surface.

Taken together, these data demonstrate that PagN is able to mediate cell invasion but regardless of the HS, suggesting that HSPG are involved but not sufficient to allow the invasion mechanism mediated by PagN-mediated invasion.

PagN-mediated internalization requires β1 integrin

According to the literature, HSPG may act as co-receptors for downstream cellular signaling events triggered by integrins [28, 29]. To assess the role of β1 integrin in PagN-

mediated invasion, cells that were deficient for β1 chain integrin production were used. F9 cells carry three copies of the gene encoding the β1 integrin chain, and TKO (triple knockout) cells fail to express β1 integrin chain due to insertions in each of the three copies. DKO (double knockout) cells retain one intact copy of the *β1 integrin* gene and thus retain production of β1 integrins [30]. Targeted deletion of β1 integrins in F9 cells affects morphological differentiation but not tissue-specific gene expression. As control, an *E. coli* MC1061 strain which overexpresses the *Yersinia Enterocolitica* Invasin protein (*MC-InvGFP*) allowing binding to β1 integrin receptor and subsequent invasion into mammalian cells was used [31]. The abillity of *HB101-pagN* and *MC-InvGFP* to bind to and invade F9, TKO and DKO cells was thus compared. As expected, Invasin-expressing strain was able to adhere and invade more efficiently cells expressing β1 integrin receptor (Figure 4). As shown in Figure 5B, the percentage of internalized *HB101-pagN* was significantly higher in F9, and DKO cells, expressing β1 integrin than in TKO cells, Indeed, an 8- and 5-fold decrease in invasion was observed in TKO cells compared to the other two cell lines, respectively. In contrast, the absence of β1 integrin resulted in similar level of the total number of cell-associated bacteria (Figure 5A). This provides evidence that PagN-mediated internalization but not adhesion depends on β1 integrin.

The involvement of β1 integrin in PagN-mediated internalization led us to investigate the cooperation of HSPG and β1 integrin in this process. To this end, the ability of *HB101-pagN* to invade pgsA745 cells pre-treated with a blocking anti-β1-chain integrin antibody or with IgG as a control was measured. As shown in Figure 5D, the pre-treatment with an anti-β1 integrin antibody significantly reduced the percentage of internalized *HB101-pagN* to a level similar to that obtained with the *HB101-psup* strain. In addition, the number of internalized *HB101-pagN* obtained in cells untreated or treated with IgG was similar. The difference observed is not due to a difference in the ability of the bacteria to adhere to cells as the pre-

treatment with either an anti-β1-chain integrin antibody or IgG resulted in similar level of the total number of cell-associated bacteria (Figure 5C). These data confirm that the internalization triggered by PagN depends on HSPG and β1 integrin.

As CHO cells allowed a high level of PagN-mediated invasion, the following experiments aimed to characterize PagN-mediated internalization were performed only with this cell line.

_S._ Typhimurium Rck- and PagN- mediated internalization hijacks the host cellular actin, leading to a Zipper mechanism.

To demonstrate that PagN alone can induce cell adhesion, actin cytoskeletal rearrangement and cell invasion, a model with 2 µm latex beads coated with PagN fused to Glutathione S-Transferase (PagN-beads) has been established and GST-coated beads were used as control. GST-PagN fusion protein was produced and purified from BL21 pLysS harboring pGEX4T2-PagN. Adhesion of PagN- and GST-coated beads to CHO cells was detected by their green autofluorescence and internalization of those beads by their double fluorescence due to labelled antibodies against GST and green autofluorescence (Table 1). Actin recruitment at the entry site was visualized using confocal microscopy. F-actin was stained with phalloidin conjugated to rhodamine (Figure 6A) and coated beads were in green due to their green autofluorescence. Confocal images were generated and showed a local actin polymerization underneath PagN-beads (Figure 6A). As expected, GST-coated beads were rarely found associated with cells as previously observed by Rosselin et al. (Table 1). As shown in Figure 6A and Table 1, PagN is able to mediate adhesion, actin rearrangement and invasion into CHO cells. These data show that PagN of *S.* Typhimurium induces adhesion and actin rearrangement, leading to bacterial invasion.

S. Typhimurium expresses two outer membrane proteins, PagN and Rck. Both induce actin polymerization, leading to bacterial internalization [10, 16]. To compare the PagN-mediated invasion process with the mechanism induced by Rck of *S.* Typhimurium, we performed several experiments to confirm that Rck of *S.* Typhimurium had the same properties as Rck of *S.* Enteritidis [10, 12, 13]. Two models were used: (i) a non-invasive *E. coli* strain, which overexpressed Rck of *S.* Typhimurium (*MC1061-rck)* and its control *E. coli* strain, only harboring pSUP202 (*MC1061-psup*) and (ii) beads coated with the 114-159 peptide of Rck fused to Glutathione S-Transferase (Rck-beads) and its control GST-beads. The peptide 114-159 of *S.* Enteritidis Rck has been shown to be sufficient and necessary to induce adhesion, actin polymerization and internalization [10]. First, the adhesion and invasion level of *MC1061-rck* and *MC1061-psup* were compared in Jeg3 cells, a cell line already shown to be permissive to Rck-mediated adhesion and invasion [10, 12]. As shown in Figure 6B-C, *MC1061-rck* strain adhered to and invaded Jeg3 cells about 6 and 300 times more efficiently, respectively, than the control *MC1061-psup* strain did. Then, we confirmed that Rck-beads could induce cell adhesion, actin cytoskeletal rearrangement and cell invasion. As observed in Table 1 and Figure 6A, Rck-beads are able to adhere and to induce host actin rearrangement or particle internalization. Taken together, our results show that bacteria expressing Rck, as well as beads coated with Rck are good models to characterize the internalization mechanism induced by Rck of *S.* Typhimurium and to compare it to the PagN-mediated invasion mechanism.

The interaction of *HB101–pagN* or the PagN-beads with CHO cell surface were further analyzed by scanning electron microscopy and compared to the membrane rearrangement observed with *MC1061-Rck* or Rck-beads incubated with Jeg3 cells. In Figure 7, the different stages of PagN- (Figure 7A-B) and Rck- (Figure 7C-D) mediated invasion can be pictured, i.e. adherent bacteria or beads associated with cellular extension membrane, partially engulfed bacteria or beads with a membrane rearrangement and totally internalized beads. The PagN-

dependent membrane rearrangements are weak and similar to the membrane engulfment observed during the Rck-mediated invasion. This suggests that PagN mediates a Zipper-like entry mechanism like the outer membrane protein Rck.

The signaling pathway induced by *S.* Typhimurium Rck- and PagN-mediated internalization, involves the PI 3-kinase pathway

The β1 integrin and Rck of *S.* Enteritidis trigger a signaling cascade involving the class I PI 3-kinase p85α-p110 heterodimer pathway [12, 32].To investigate the specificity of this signaling cascade with regard to the mechanism induced by PagN and Rck of *S.* Typhimurium, the effect of the p110 heterodimer inhibitor (AS-604850) on adhesion and entry of *HB101–pagN* and *MC1061-rck* was examined. Addition of AS-604850 to CHO and Jeg3 cell monolayers before adherence and invasion assays had no effect on adhesion as the number of associated *HB101-pagN* and *MC1061-rck* bacteria were similar that of DMSO-treated cells (Figure 8A-C). However, the number of internalized Rck-expressing bacteria decreased in a dose-dependent manner with this inhibitor. Similar results were observed with PagN-expressing bacteria (Figure 8B-D).

To obtain clear evidence that the class I PI 3-kinase p85α-p110 is needed for the invasion mechanism induced by PagN and Rck of *S.* Typhimurium, the dominant negative form of p85α (Δp85α) and the wild-type form of p85α (Wp85α) were stably overexpressed in CHO and Jeg3 cells. 35 amino acids from residues 479-513 of p85α are deleted in the dominant negative form, known to inhibit PI 3-kinase activation [12, 33]. The ability of *HB101-pagN* and *MC1061-rck* to bind to and invade these stably transfected cells was thus compared. As shown in Figure 8E-H, the number of internalized bacteria expressing either PagN or Rck was significantly lower in Δp85α cells, compared to that in Wp85α cells, while no significant change was highlighted in the number of cell-associated bacteria between the transfected cell lines.

These results indicate that the p85α-p110 heterodimer plays a role in the signaling pathway induced by both PagN and Rck, leading to bacterial internalization into cultured cells.

Activation of the PI 3-kinase requires the interaction of the SH2 domains of the p85 subunit with tyrosine phosphorylated proteins [34]. To assess the role of protein tyrosine kinases in *S.* Typhimurium PagN- or Rck- mediated internalization, the effect of treatment with genistein, a specific inhibitor of protein tyrosine kinases, was analyzed on PagN or Rck-mediated adhesion and internalization. As shown in Figure 9, the PagN- or Rck-mediated invasion decreased in the presence of genistein in a dose-dependent manner, whereas no effect on PagN- or Rck-mediated adhesion was highlighted. These results show that the PagN- or Rck-dependent internalization mechanism requires tyrosine phosphorylation.

Taken together, these data demonstrate that like for Rck invasion, PagN of *S.* Typhimurium induces and requires the PI 3-kinase signaling pathway to trigger bacterial internalization.

Discussion

S. Typhimurium takes advantage of different strategies to invade host cells. The major determinant of this invasiveness described in the literature is the T3SS-1, but other T3SS-independent mechanisms are also used by *S.* Typhimurium to gain entry into host cells such as the outer membrane proteins, Rck and PagN. Our study aimed to characterize better PagN and the entry pathway induced by this outer membrane protein. Previously, the presence of the *pagN* ORF was studied in few strains or genomes and this ORF was shown to be present in all the strains tested [19, 21, 24]. Based on Enterobase, we were able to confirm the presence of the *pagN* ORF on a very large dataset of more than 188,000 genomes of *Salmonella,* including genomes of the two *Salmonella* species, i.e. *S. bongori* and *S. enterica,* of all *S. enterica* subspecies and of 465 different serovars of *S. enterica* subsp. *enterica*. More than 99.6 % of the

tested genomes were positive for the gene, confirming studies based on a more limited number of strains/genomes. Moreover, for the first time, we highlighted some allelic specificity at the species, subspecies and serovar levels. Despite this allelic specificity, allelic variants show a very high conservation within *S. enterica* subsp. *enterica*, and also within other subspecies and species but to a lower extent. This high conservation does not, however, predict the functionality of the protein as it has recently been shown that only one substitution in loop 1 or 2 could be sufficient to increase the adhesive and invasive properties of PagN [35]. Further studies are required to decipher the amino acids/peptides important for PagN function, especially those in the predicted outer membrane loops.

Based on several lines of evidence, Lambert and Smith indicated that the epithelial cell surface receptor of PagN may be a HSPG [17]. They showed that *S.* Typhimurium and recombinant *E. coli* expressing PagN had a significant decrease in the ability to invade cells presenting under-glycosylated proteoglycans and that PagN-mediated internalization was significantly reduced in cells pre-treated with exogenous glycosaminoglycans and heparin. In our study, we compared the level of PagN-mediated invasion in different cell lines and identified them as permissive, resistant, and intermediate cells to this invasion process. However, the quantification of HS, which occurs as HSPG, on the surface of cells of these lines did not allow us to establish a link with the permeability/resistance of the cells to PagN-mediated invasion. Indeed, HT29 cells, which are extremely resistant to PagN-mediated invasion, express the highest amount of HS on their surface compared to the other cell lines tested. Therefore, the susceptibility/resistance to the PagN-mediated invasion is not proportional to the distribution of HS on these cell lines. As the PagN-mediated invasion is reduced in HSPG deficient cells compared to parental cells, all these results suggest that HSPG are necessary but not sufficient for *S.* Typhimurium internalization and thus could be considered as a co-receptor in PagN-mediated invasion.

375 The literature describes clearly that HSPG can be conjugated onto a variety of proteins
376 to induce a signaling pathway, allowing the invagination of the cell membrane. Exosomes, cell
377 penetrating peptides, viruses, bacteria, growth factors, lipoproteins and morphogens among
378 other ligands penetrate cells through HSPG-mediated endocytosis. This leads to the modulation
379 of biological activities of these molecules by influencing the duration and potency of the
380 signaling. HSPG may thus act as a co-receptor for different cell surface receptors. The ligand-
381 binding to HSPG results in conformational change of ligand, allowing it to present to
382 endocytosis receptors with a high-affinity [36]. HSPG endocytosis seems thus not to be limited
383 to one particular pathway, and changes depending on the type of extracellular ligand and
384 cellular context. HSPG are exclusively produced by epithelial cells [37] and they have been
385 detected in the intestine of humans [38] and mice [39]. Binding to host cells through recognition
386 of HSPG has been associated with the invasion of several bacteria such as *Neisseria*
387 *gonorrhoeae* [40]. Syndecan-1 and -4 are involved in attachment of host cells by *Neisseria*
388 *gonorrhoeae* [41, 42], acting as co-receptor to facilitate bacterial internalization thanks to the
389 β1 integrin receptor [43]. Syndecan-1 is a highly conserved, multifunctional receptor and the
390 major HSPG expressed on intestinal epithelial cell surfaces [44]. As Syndecan-1 and β1 integrin
391 generate a signal via the PI 3-kinase pathway [45] and undergo endocytosis upon clustering
392 [46], our results reinforce the observation of Lambert and Smith [17], suggesting that Syndecan-
393 1 is involved in the PagN-mediated internalization mechanism.
394 Signaling molecules are differentially targeted by bacteria to promote invasion. During
395 Zipper bacterial invasion, the receptor-ligand interaction leads to a PI 3-kinase signaling
396 pathway and the stimulation of actin cytoskeletal rearrangements, promoting the advance of
397 pseudopods [47]. In this study, the signaling pathway induced by *S.* Typhimurium Rck and
398 PagN, leading to bacterial internalization was characterized and compared to elucidate when
399 the bacteria use these two outer membrane proteins. Using a pharmacological inhibitor and a

dominant negative mutant of class I PI 3-kinase, we demonstrated in this study that the signaling transduction induced by *S.* Typhimurium Rck requires (p85-p110) PI 3-kinase as Rck of *S.* Enteritidis. In addition, the use of these tools also allowed us to show that (p85-p110) PI 3-kinase is required for the signaling transduction which leads to PagN-mediated invasion without affecting attachment.

As protein tyrosine kinase is an upstream signaling molecule of (p85-p110) PI 3-kinase during the Rck-mediated internalization of *S.* Enteritidis, the involvement of protein tyrosine kinase in PagN- and Rck-mediated invasion of *S.* Typhimurium was investigated. Our data highlighted that phosphorylation of tyrosine is required for the Rck- and PagN-mediated invasion by showing that the invasion level induced by Rck or PagN was significantly reduced in cells treated with the inhibitor genistein. Our data demonstrate that the signaling induced by Rck- and PagN-mediated entry of *S.* Typhimurium has similarities and involves the PI 3-kinase pathway, to allow bacterial internalization.

The scanning electron microscopy analysis of the interaction between either *HB101-pagN* or PagN-beads and epithelial host cell surface revealed a Zipper-like structure surrounding the adherent bacteria and coated beads. These data, combined with the fact that (i) β1 integrin is required for PagN-mediated internalization and has been described in the literature as a receptor, allowing Zipper-like process and (ii) PagN alone mediates a PI 3-kinase signaling pathway, leading to internalization, strongly suggest that PagN and Rck of *S.* Typhimurium trigger cell invasion through a Zipper-like mechanism, as during Rck-mediated internalization of *S.* Enteritidis [10].

The transcription of *pagN* is directly regulated by PhoP/PhoQ [48].This two-component system is activated by an acidified environment and a low Mg^{2+} concentration, conditions found intracellularly, inside the *Salmonella*-containing vacuole (SCV). By contrast, this environmental condition is not favorable for Rck production (data not shown). Currently, Rck

425 production is known to be directly regulated by SdiA in an AHL–dependent manner [8, 49]
426 despite the fact that some studies have shown that *Salmonella* does not produce AHLs and that
427 some evidence suggests a lack of AHL signaling molecules in the mammalian intestine [15,
428 50]. In addition, the genes encoding T3SS-1 are induced extracellularly (by high osmolarity
429 and low oxygen concentration) and downregulated after internalization [51, 52]. Altogether,
430 these data show that *S.* Typhimurium expresses and uses its invasion factors under different
431 environmental conditions, suggesting a specificity of the entry route by *Salmonella* strains
432 which depends on the host cell environment.

433 In *Salmonella* pathogenicity, the importance of Rck- and PagN- mediated invasion
434 remains unknown. *In vivo* studies in mice suggest an intestinal role of PagN and Rck [15, 21,
435 23] and lead to several hypotheses. In the intestine, EGFR, HSPG and β1 integrins are present
436 on the surface of epithelial cells constituting the intestinal crypt base [53]. As *Salmonella* can
437 target intestinal stem cells [54], Rck- and PagN- mediated invasion could occur at the lumen
438 site of the crypts. In addition, M cells express β1 integrins on their luminal side [55]. *Salmonella*
439 is able to invade and destroy M cells, leading to invasion and colonization of the intestine [56].
440 As a *Salmonella* strain with a nonfunctional T3SS-1 is still able to invade M cells in mouse
441 intestine, it is possible that the PagN-mediated invasion may be targeting M cells [57-59].
442 Moreover, EGFR, HSPG and β1 integrins are found to be expressed on the basolateral
443 membrane of villus enterocytes [60-62]. As *Salmonella* can cross the intestinal barrier and exit
444 on the basolateral side [63, 64], one hypothesis could be that Rck and PagN allow *Salmonella*
445 invasion of enterocytes via the basolateral side. Based on the fact that *Salmonella* uses its T3SS-
446 1 to alter epithelial cell polarity to allow bacterial invasion, another possibility thus could be
447 that initial *Salmonella* invasion on the apical side induces a redistribution of HSPG, β1 integrins
448 and EGFR on the cell surface, allowing PagN- and Rck- mediated invasion from the apical side
449 of epithelium [65].

Salmonella colonization is not limited to the intestinal tract. Indeed, *Salmonella* can disseminate and colonize systemic sites [66]. Considering that (i) a *S.* Typhimurium strain with a non fonctionnel T3SS-1 is still be able to infect mice and colonize systemic organs such as the liver [67], (ii) *Salmonella* colonization of mice liver is significantly reduced in absence of PagN [21, 23], (iii) EGFR and β1 integrins are expressed on the cell surface of hepatocytes [68, 69], another hypothesis could be that PagN- and Rck-mediated invasion allow the bacterial colonization of systemic organs such as the liver. The fact that Rck confers resistance to complement-mediated killing, reinforces this hypothesis [70]. The next step now is to investigate these different hypotheses using organoid models as a primary intestinal epithelium *in vitro* culture model.

Conclusions

Overall, the comparison of PagN- and Rck- mediated invasion of *S.* Typhimurium highly indicates that PagN induces a phosphatidylinositol 3-kinase signaling pathway, leading to a Zipper-like entry mechanism as the *Salmonella* outer membrane protein Rck. The investigation of the molecular elements of the signal transduction mediated by PagN supplies new comprehensions into T3SS-1-independent invasion mechanisms and could help to explain the specificity of each internalization process pathway.

Methods

Bioinformatics analyses

We retrieved the wgMLST profiles of 195,555 *Salmonella* strains recorded in Enterobase, an online platform that assembles draft genomes from Illumina short reads [71] on March 27, 2019. Among these strains, we kept only those presenting consistent serovar predictions (obtained using the online typing tool SISTR [72]. Consequently, the analysis was performed on 188,233

genomes. Allelic data at the *pagN* locus (referred to as STMMW_03171 in Enterobase's wgMLST scheme) were retrieved from the dataset and the distribution of the alleles was studied according to the *Salmonella* species, subspecies and serovars. The diversity among nucleotide sequences was calculated at each taxonomic level (species, subspecies and serovar) using Nei's haplotypic diversity (Hd), computed using the R-package pegas [73, 74]. After translation, sequences were aligned with the protein encoded by allele designated as No. 1 in Enterobase using ClustalW implemented in the software Geneious 10.2.2 (https://www.geneious.com).

Cell lines and Reagents. Various mammalian cell lines were used in this study. Parental F9, and integrin β1 double (DKO) and triple (TKO) knockout F9 embryonal carcinoma cell lines (kindly provided by Dr. C. Le Bouguenec, Institut Pasteur Paris, France) as well as Chinese Hamster Ovary (CHO) cells (ATCC: CCL-61) and HT29 cells, human caucasian colon adenocarcinoma cells (ATCC: HTB-38) were cultured in DMEM (Dulbecco's modified Eagle's medium, Gibco) containing glucose 25 mM supplemented with FBS 10 % (fetal bovine serum; Sigma), L-glutamine 2 mM (Gibco) in a humidified atmosphere at 37 °C and CO_2 5 %. Jeg-3 cells, human epithelial placental cells (ATCC: HTB-36), and the stably transfected cells, Jeg-3 Wp85α and Δp85α, were grown in MEM medium containing Glutamax (Gibco), FBS 10 %, non-essential amino acids 1 mM and sodium pyruvate 1 mM (Gibco; [12]). Caco-2 cells (ATCC: HTB-37) are human colonic epithelial cell lines cultured in DMEM supplemented with FBS 20 %, nonessential amino acids 1 mM, sodium pyruvate 1 mM and L-glutamine 2 mM. pgsA745 cells (ATCC : CRL-2242) referred to as Δ*XylT* [75] were routinely cultured in F-12K medium (Kaighn's Modification of Ham's F-12 medium ; ATCC) supplemented with FBS10 %.

All inhibitors were dissolved in DMSO (dimethyl sulfoxide, Sigma) at the following stock concentration: AS604850 (Sigma at 35 mM); Genistein (Calbiochem at 100 mM). In drug-treated cells, the maximum final concentration of DMSO never exceeded 0.1% (v/v).

Bacterial strains and growth conditions. In Table 2, the bacterial strains used in this study are listed. Bacteria were routinely cultured in LB (Luria-Bertani) broth overnight with shaking at 150 rpm at 37°C with the corresponding antibiotic: tetracyclin (Tc, Sigma) 12.5 µg/ml, chloramphenicol (Cm, Sigma) 34 µg/ml and carbenicillin (Cb, Sigma) 100 µg/ml.

Expression of Wp85α and mutant Δp85α in CHO cells. CHO cells stably overexpressing Wp85α or Δp85α were obtained as described by Mijouin et al [12]. Selection was started by adding G-418 at 1 mg/ml to the cell culture medium. For pcDNA3.1 and Rev pcDNA3.1 primers (listed in Table 3) were used to screen by polymerase chain reaction (PCR) the resistant CHO cells expressing each protein. Proliferation of Wp85α and mutant Δp85α CHO cells was similar as described previously [12].

DNA constructs. The *pagN* gene was amplified from wild-type *S.* Typhimurium 14028 strain by PCR (polymerase chain reaction) using *pagN* EcoRI forw primer (flanked by EcoRI restriction site) and *pagN* NcoI rev primer (flanked by NcoI restriction site) and cloned into pSUP202 expression vector [76], before being transformed into *E. coli* HB101. The same method was used to construct the $(His)_6$-*pagN* without its signal peptide (PagN-GST) into pGEX-4T-2 expression vector (Amersham-Pharmacia), using primers *pagN*-GST forw and *pagN*-GST rev, flanked by BamHI and EcoRI restriction sites, before being transformed into *E. coli* BL21 pLysS. In Table 3, primer sequences used in this study are listed.

524

525 **Adhesion and invasion assays.** Cells were cultured in 24-well tissue culture plates (Falcon) to
526 obtain a confluent monolayer. They were infected for 60 min at 37°C with bacteriain DMEM
527 without FBS.

528 For adhesion assays, after infection, cells were washed at least four times with PBS
529 (phosphate buffer saline, Sigma) and then lysed at 4°C with distilled water. Viable bacteria
530 (extra- and intra-cellular) were counted after plating serial dilutions on TSA (Tryptic Soy Agar).

531 The number of internalized bacteria was determinated using a gentamicin protection
532 assay to kill extracellular bacteria, as previously described [11]. After 90 min treatment with
533 gentamicin at 100 µg/ml (Gibco), cells were washed and lysed in cold distilled water. The
534 number of internalized bacteria was enumerated as before [11].

535

536 **Flow cytometry.** The CHO, pgsA745, HT29 and Caco2 cells were fixed for 15 min in PFA 2
537 % (paraformaldehyde) at 4 °C and then washed with cold wash buffer containing BSA at 0.5
538 % (bovine serum albumin). Cell samples were saturated with PBS containing BSA 2.5 % at 4
539 °C for 15 min. The mouse anti-heparin/heparan sulfate (HS; clone T320.11, Millipore) was
540 diluted to 1:40 in PBS containing BSA 1 % and incubated with cells for 45 min on ice and then
541 washed three times. As the secondary antibody, Alexa 488-conjugated goat anti–mouse
542 antibodies (Invitrogen) diluted to 1:200 in PBS containing BSA 1 % were used and incubated
543 with cells for 45 min on ice. After three washes, cells were resuspended in PFA 2 % and then
544 the relative fluorescence of the cell lines was analyzed using a LSR-Fortessa X-20 analyzer
545 (BD Biosciences). The relative surface expression of HS on cells is expressed as the percentage
546 of positive cells (determined by Overton subtraction of isotype control histograms from labelled
547 histograms [77]).

548

549 **Expression and purification of recombinant protein.** Recombinant GST-tagged PagN and
550 114-159 Rck proteins were induced in *E. coli* BL21 pLysS transformed with pGEX4T2-PagN
551 or pGEX4T2-114-159 Rck upon treatment with IPTG 1 mM (isopropyl β-D-1-
552 thiogalactopyranoside, Sigma) for 4 h as previously described [10]. For protein purification,
553 cells were harvested by centrifugation, resuspended in buffer containing Tris pH 8 50 mM,
554 EDTA40 mM, sucrose 25 %, $MgCl_2$ 100 mM, Triton X-100 0.2 %, PMSF
555 (phenylmethylsulfonylfluoride) 1 mM and cOmplete Protease Inhibitor Cocktail (Boehringer)
556 and sonicated. After clearing, fusion proteins were affinity-purified from the soluble fraction
557 on Glutathione-Sepharose 4B beads (Amersham Biosciences) following the manufacturer's
558 instructions [10].
559
560 **Coating of latex beads.** 2 µm diameter latex beads (polystyrene sulphate modified, Sigma)
561 were washed and resuspended in PBS containg purified GST-114-159 Rck, GST-PagN and
562 GST proteins. Proteins were adsorbed onto the beads at room temperature for 3 h. After adding
563 BSA (20 mg/ml), the beads were incubated for a further hour at room temperature. The beads
564 were then washed in PBS.
565
566 **Immunofluorescence microscopy.** Jeg-3 and CHO cells on coverslips were infected with
567 either GST-114-159 Rck-, GST-PagN- or GST- coated beads at MOI 50:1. After incubation
568 for 30 min, cells were washed in PBS to remove unbound extracellular beads. In brief, after
569 fixation of the monolayers in PFA 4 %, and permeabilization in triton 0.2 %, actin was stained
570 with Rhodamin-Phalloidin (diluted 1:200; Sigma;). Finally, coverslips were mounted in
571 fluorescence mounting medium (Dako) and analyzed with a Leica SP8 confocal laser-scanning
572 microscope (Leica TCS SP8, Germany).
573

Scanning Electron microscopy. CHO and Jeg3 cells were grown on coverslips and infected with beads or bacteria to a cell ratio of 100:1. After 30 min of bacteria- or beads- cell contact at 37 °C, cells were washed in PBS and fixed in a mixture of PFA 4 % and glutaraldehyde 1 % (0.3 M pH 7.4) for 1 h. Samples were then treated for scanning electron microscopy analysis as described in Burlaud-Gaillart *et al*. [78].The observations were performed using a Zeiss Ultra plus FEG-SEM scanning electron microscope (Oberkochen, Germany).

Statistical analysis. Data were analyzed using an unpaired t test or a Mann Whitney test using Prism (version 6.0; GraphPad Software, La Jolla, CA, USA).

Abbreviations

AHL: N-acyl-L homoserine lactones

BSA: bovine serum albumine

Cb: carbenicillin

Cm: chloramphenicol

DKO: integrin β1 double knockout

DMEM: Dulbecco's modified Eagle's medium

DMSO: dimethyl sulfoxide

EGFR: epidermal growth factor receptor

FBS: fetal bovine serum

GST: Glutathione S-Transferase

Hd: haplotype diversity

HS: heparan sulphates

HSPG: heparan sulfate proteoglycan

IPTG: isopropyl β-D-1-thiogalactopyranoside

LB: Luria-Bertani

MOI: multiplicity of infection

PAF: paraformaldehyde

PagN: *phoP*-activated gene

PBS: phosphate buffer saline

PCR: polymerase chain reaction

PI 3-kinase: phosphatidylinositol 3-kinase

PMSF: phenylmethylsulfonylfluoride

Rck: resistance to complement killing

R: Richness

SCV: *Salmonella*-containing vacuole

SPI-1: *Salmonella* pathogenicity island-1

Tc: tetracyclin

TKO: integrin β1 triple knockout

T3SS-1: type III secretion system-1

TSA: tryptic soy agar

Declaration

Ethics approval and consent to participate

Not applicable

Consent for publication

All the authors read and approved the final manuscript.

Availability of data and materials

The datasets used to produce the results in Figure 1 are publically available in Enterobase. The analysis is available from Olivier Grépinet (olivier.grepinet@inrae.fr).

Competing interests

The authors declare that they have no competing interests.

Funding

This work was supported by the ERA-NET InfectERA (SalHostTrop, ANR-15-IFEC-0003).

Acknowledgements

The authors thank Dr. C. C. Le Bouguenec, Institut Pasteur Paris, France for donating F9, TKO and DKO cells and Y. Le Vern for flow cytometry expertise.

Author Contributions

AW designed the research; EB, MV, MK, JBG and AW performed research; FK contributed analytic tools; AW, MV, MK, FK, OG, IVP and EB analyzed data; AW wrote the manuscript; PV provided critical comments.

References

1. Guibourdenche M, Roggentin P, Mikoleit M, Fields PI, Bockemuhl J, Grimont PA *et al*. Supplement 2003-2007 (No. 47) to the White-Kauffmann-Le Minor scheme. Res Microbiol. 2010;161(1):26-9.
2. Velge P, Wiedemann A, Rosselin M, Abed N, Boumart Z, Chausse AM *et al*. Multiplicity of *Salmonella* entry mechanisms, a new paradigm for *Salmonella* pathogenesis. MicrobiologyOpen. 2012;1(3):243-58.

3. McClelland M, Sanderson KE, Spieth J, Clifton SW, Latreille P, Courtney L *et al*. Complete genome sequence of *Salmonella enterica* serovar Typhimurium LT2. Nature. 2001;413(6858):852-6.

4. Hume PJ, Singh V, Davidson AC, Koronakis V. Swiss army pathogen: The *Salmonella* entry toolkit. Front Cell Infect Microbiol. 2017;7:348.

5. Lou L, Zhang P, Piao R, Wang Y. *Salmonella* Pathogenicity Island 1 (SPI-1) and its complex regulatory network. Front Cell Infect Microbiol. 2019;9:270.

6. Mambu J, Virlogeux-Payant I, Holbert S, Grepinet O, Velge P, Wiedemann A. An updated view on the Rck invasin of *Salmonella*: still much to discover. Front Cell Infect Microbiol. 2017;7:500.

7. Ahmer BM, van Reeuwijk J, Timmers CD, Valentine PJ, Heffron F. *Salmonella typhimurium* encodes an SdiA homolog, a putative quorum sensor of the LuxR family, that regulates genes on the virulence plasmid. J Bacteriol. 1998;180(5):1185-93.

8. Abed N, Grepinet O, Canepa S, Hurtado-Escobar GA, Guichard N, Wiedemann A *et al*. Direct regulation of the *pefI-srgC* operon encoding the Rck invasin by the quorum-sensing regulator SdiA in *Salmonella* Typhimurium. Mol Microbiol. 2014;94(2):254-71.

9. Erickson DL, Nsereko VL, Morgavi DP, Selinger LB, Rode LM, Beauchemin KA. Evidence of quorum sensing in the rumen ecosystem: detection of N-acyl homoserine lactone autoinducers in ruminal contents. Can J Microbiol. 2002;48(4):374-8.

10. Rosselin M, Virlogeux-Payant I, Roy C, Bottreau E, Sizaret PY, Mijouin L *et al*. Rck of *Salmonella enterica*, subspecies enterica serovar Enteritidis, mediates Zipper-like internalization. Cell research. 2010;20(6):647-64.

11. Wiedemann A, Mijouin L, Ayoub MA, Barilleau E, Canepa S, Teixeira-Gomes AP *et al*. Identification of the epidermal growth factor receptor as the receptor for *Salmonella* Rck-dependent invasion. FASEB J. 2016;30(12):4180-91.

12. Mijouin L, Rosselin M, Bottreau E, Pizarro-Cerda J, Cossart P, Velge P *et al*. *Salmonella enteritidis* Rck-mediated invasion requires activation of Rac1, which is dependent on the class I PI 3-kinases-Akt signaling pathway. FASEB J. 2012;26(4):1569-81.
13. Wiedemann A, Rosselin M, Mijouin L, Bottreau E, Velge P. Involvement of c-Src tyrosine kinase upstream of class I phosphatidylinositol (PI) 3-kinases in *Salmonella* Enteritidis Rck protein-mediated invasion. J Biol Chem. 2012;287(37):31148-54.
14. Mambu J, Barilleau E, Fragnet-Trapp L, Le Vern Y, Olivier M, Sadrin G *et al*. Rck of *Salmonella* Typhimurium delays the host cell cycle to facilitate bacterial invasion. Front Cell Infect Microbiol. 2020;10:586934.
15. Dyszel JL, Smith JN, Lucas DE, Soares JA, Swearingen MC, Vross MA *et al*. *Salmonella enterica* serovar Typhimurium can detect acyl homoserine lactone production by in mice. J Bacteriol. 2010;192(1):29-37.
16. Lambert MA, Smith SG. The PagN protein of *Salmonella enterica* serovar Typhimurium is an adhesin and invasin. BMC Microbiol. 2008;8:142.
17. Lambert MA, Smith SG. The PagN protein mediates invasion via interaction with proteoglycan. FEMS Microbiol Lett. 2009;297(2):209-16.
18. Belden WJ, Miller SI. Further characterization of the PhoP regulon: identification of new PhoP-activated virulence loci. Infect Immun. 1994;62(11):5095-101.
19. Folkesson A, Advani A, Sukupolvi S, Pfeifer JD, Normark S, Lofdahl S. Multiple insertions of fimbrial operons correlate with the evolution of *Salmonella* serovars responsible for human disease. Mol Microbiol. 1999;33(3):612-22.
20. Rakov AV, Mastriani E, Liu SL, Schifferli DM. Association of *Salmonella* virulence factor alleles with intestinal and invasive serovars. BMC Genomics. 2019;20(1):429.
21. Yang Y, Wan C, Xu H, Aguilar ZP, Tan Q, Xu F *et al*. Identification of an outer membrane protein of *Salmonella enterica* serovar Typhimurium as a potential vaccine candidate for Salmonellosis in mice. Microbes and infection / Institut Pasteur. 2013;15(5):388-98.

699 22. Kato A, Groisman EA, Howard Hughes Medical I. The PhoQ/PhoP regulatory network of
700 *Salmonella enterica*. Adv Exp Med Biol. 2008;631:7-21.
701 23. Conner CP, Heithoff DM, Mahan MJ. *In vivo* gene expression: contributions to infection,
702 virulence, and pathogenesis. Curr Top Microbiol Immunol. 1998;225:1-12.
703 24. Suez J, Porwollik S, Dagan A, Marzel A, Schorr YI, Desai PT *et al*. Virulence gene profiling and
704 pathogenicity characterization of non-typhoidal *Salmonella* accounted for invasive disease in
705 humans. PLoS One. 2013;8(3):e58449.
706 25. EFSA. The European Union summary report on trends and sources of zoonoses, zoonotic
707 agents and food-borne outbreaks in 2017. EFSA J. 2018;16(12):5500.
708 26. Annaval T, Wild R, Cretinon Y, Sadir R, Vives RR, Lortat-Jacob H. Heparan sulfate proteoglycans
709 biosynthesis and post synthesis mechanisms combine few enzymes and few core proteins to
710 generate extensive structural and functional diversity. Molecules. 2020;25(18).
711 27. Finlay BB, Falkow S. *Salmonella* interactions with polarized human intestinal Caco-2 epithelial
712 cells. J Infect Dis. 1990;162(5):1096-106.
713 28. Montgomery AM, Becker JC, Siu CH, Lemmon VP, Cheresh DA, Pancook JD *et al*. Human neural
714 cell adhesion molecule L1 and rat homologue NILE are ligands for integrin α_v β_3. J Cell Biol.
715 1996;132(3):475-85.
716 29. Schlessinger J, Lax I, Lemmon M. Regulation of growth factor activation by proteoglycans: what
717 is the role of the low affinity receptors? Cell. 1995;83(3):357-60.
718 30. Stephens LE, Sonne JE, Fitzgerald ML, Damsky CH. Targeted deletion of β_1 integrins in F9
719 embryonal carcinoma cells affects morphological differentiation but not tissue-specific gene
720 expression. J Cell Biol. 1993;123(6 Pt 1):1607-20.
721 31. Isberg RR, Leong JM. Multiple beta 1 chain integrins are receptors for invasin, a protein that
722 promotes bacterial penetration into mammalian cells. Cell. 1990;60(5):861-71.
723 32. Pellinen T, Ivaska J. Integrin traffic. J Cell Sci. 2006;119(Pt 18):3723-31.

33. Hara K, Yonezawa K, Sakaue H, Ando A, Kotani K, Kitamura T *et al*. 1-Phosphatidylinositol 3-kinase activity is required for insulin-stimulated glucose transport but not for RAS activation in CHO cells. Proc Natl Acad Sci USA. 1994;91(16):7415-9.
34. Cantley LC. The phosphoinositide 3-kinase pathway. Science. 2002;296(5573):1655-7.
35. Wu Y, Hu Q, Dehinwal R, Rakov AV, Grams N, Clemens EC *et al*. The Not so Good, the Bad and the Ugly: Differential bacterial adhesion and invasion mediated by *Salmonella* PagN allelic variants. Microorganisms. 2020;8(4).
36. Christianson HC, Belting M. Heparan sulfate proteoglycan as a cell-surface endocytosis receptor. Matrix Biol. 2014;35:51-5.
37. Simon-Assmann P, Bouziges F, Vigny M, Kedinger M. Origin and deposition of basement membrane heparan sulfate proteoglycan in the developing intestine. J Cell Biol. 1989;109(4 Pt 1):1837-48.
38. Oshiro M, Ono K, Suzuki Y, Ota H, Katsuyama T, Mori N. Immunohistochemical localization of heparan sulfate proteoglycan in human gastrointestinal tract. Histochem Cell Biol. 2001;115(5):373-80.
39. Bode L, Salvestrini C, Park PW, Li JP, Esko JD, Yamaguchi Y *et al*. Heparan sulfate and syndecan-1 are essential in maintaining murine and human intestinal epithelial barrier function. J Clin Invest. 2008;118(1):229-38.
40. van Putten JP, Paul SM. Binding of syndecan-like cell surface proteoglycan receptors is required for *Neisseria gonorrhoeae* entry into human mucosal cells. EMBO J. 1995;14(10):2144-54.
41. Alvarez-Dominguez C, Vazquez-Boland JA, Carrasco-Marin E, Lopez-Mato P, Leyva-Cobian F. Host cell heparan sulfate proteoglycans mediate attachment and entry of *Listeria monocytogenes*, and the listerial surface protein ActA is involved in heparan sulfate receptor recognition. Infect Immun. 1997;65(1):78-88.

748 42. Freissler E, Meyer auf der Heyde A, David G, Meyer TF, Dehio C. Syndecan-1 and syndecan-4
749 can mediate the invasion of Opa_{HSPG}-expressing *Neisseria gonorrhoeae* into epithelial cells. Cell
750 Microbiol. 2000;2(1):69-82.
751 43. van Putten JP, Duensing TD, Cole RL. Entry of OpaA+ gonococci into HEp-2 cells requires
752 concerted action of glycosaminoglycans, fibronectin and integrin receptors. Mol Microbiol.
753 1998;29(1):369-79.
754 44. Gondelaud F, Ricard-Blum S. Structures and interactions of syndecans. FEBS J.
755 2019;286(15):2994-3007.
756 45. Yongchaitrakul T, Manokawinchoke J, Pavasant P. Osteoprotegerin induces osteopontin via
757 syndecan-1 and phosphoinositol 3-kinase/Akt in human periodontal ligament cells. J Periodont
758 Res. 2009;44(6):776-83.
759 46. Chen K, Williams KJ. Molecular mediators for raft-dependent endocytosis of syndecan-1, a
760 highly conserved, multifunctional receptor. J Biol Chem. 2013;288(20):13988-99.
761 47. Cossart P, Sansonetti PJ. Bacterial invasion: the paradigms of enteroinvasive pathogens.
762 Science. 2004;304(5668):242-8.
763 48. Gunn JS, Belden WJ, Miller SI. Identification of PhoP-PhoQ activated genes within a duplicated
764 region of the *Salmonella typhimurium* chromosome. Microb Pathog. 1998;25(2):77-90.
765 49. Smith JN, Ahmer BM. Detection of other microbial species by *Salmonella*: expression of the
766 SdiA regulon. J Bacteriol. 2003;185(4):1357-66.
767 50. Swearingen MC, Sabag-Daigle A, Ahmer BM. Are there acyl-homoserine lactones within
768 mammalian intestines? J Bacteriol. 2013;195(2):173-9.
769 51. Boddicker JD, Jones BD. Lon protease activity causes down-regulation of *Salmonella*
770 pathogenicity island 1 invasion gene expression after infection of epithelial cells. Infect Immun.
771 2004;72(4):2002-13.

52. Ibarra JA, Knodler LA, Sturdevant DE, Virtaneva K, Carmody AB, Fischer ER *et al*. Induction of *Salmonella* pathogenicity island 1 under different growth conditions can affect *Salmonella*-host cell interactions i*n vitro*. Microbiology (Reading, England). 2010;156(Pt 4):1120-33.

53. Meran L, Baulies A, Li VSW. Intestinal Stem Cell Niche: The Extracellular Matrix and Cellular Components. Stem Cells Int. 2017;2017:7970385.

54. Liu X, Lu R, Wu S, Sun J. *Salmonella* regulation of intestinal stem cells through the Wnt/beta-catenin pathway. FEBS Lett. 2010;584(5):911-6.

55. Clark MA, Hirst BH, Jepson MA. M-cell surface beta1 integrin expression and invasin-mediated targeting of Yersinia pseudotuberculosis to mouse Peyer's patch M cells. Infect Immun. 1998;66(3):1237-43.

56. Jones BD, Ghori N, Falkow S. *Salmonella typhimurium* initiates murine infection by penetrating and destroying the specialized epithelial M cells of the Peyer's patches. J Exp Med. 1994;180(1):15-23.

57. Clark MA, Reed KA, Lodge J, Stephen J, Hirst BH, Jepson MA. Invasion of murine intestinal M cells by *Salmonella typhimurium inv* mutants severely deficient for invasion of cultured cells. Infect Immun. 1996;64(10):4363-8.

58. Jensen VB, Harty JT, Jones BD. Interactions of the invasive pathogens *Salmonella typhimurium, Listeria monocytogenes,* and *Shigella flexneri* with M cells and murine Peyer's patches. Infect Immun. 1998;66(8):3758-66.

59. Martinez-Argudo I, Jepson MA. *Salmonella* translocates across an in vitro M cell model independently of SPI-1 and SPI-2. Microbiology (Reading). 2008;154(Pt 12):3887-94.

60. Beaulieu JF. Differential expression of the VLA family of integrins along the crypt-villus axis in the human small intestine. J Cell Sci. 1992;102 (Pt 3):427-36.

61. Esclatine A, Bellon A, Michelson S, Servin AL, Quero AM, Geniteau-Legendre M. Differentiation-dependent redistribution of heparan sulfate in epithelial intestinal Caco-2 cells leads to basolateral entry of cytomegalovirus. Virology. 2001;289(1):23-33.

62. Singh B, Coffey RJ. Trafficking of epidermal growth factor receptor ligands in polarized epithelial cells. Annu Rev Physiol. 2014;76:275-300.

63. Criss AK, Casanova JE. Coordinate regulation of *Salmonella enterica* serovar Typhimurium invasion of epithelial cells by the Arp2/3 complex and Rho GTPases. Infect Immun. 2003;71(5):2885-91.

64. Muller AJ, Kaiser P, Dittmar KE, Weber TC, Haueter S, Endt K *et al*. *Salmonella* gut invasion involves TTSS-2-dependent epithelial traversal, basolateral exit, and uptake by epithelium-sampling lamina propria phagocytes. Cell Host Microbe. 2012;11(1):19-32.

65. Zhang YG, Wu S, Xia Y, Sun J. *Salmonella* infection upregulates the leaky protein claudin-2 in intestinal epithelial cells. PLoS One. 2013;8(3):e58606.

66. Vazquez-Torres A, Jones-Carson J, Baumler AJ, Falkow S, Valdivia R, Brown W *et al*. Extraintestinal dissemination of *Salmonella* by CD18-expressing phagocytes. Nature. 1999;401(6755):804-8.

67. Coombes BK, Coburn BA, Potter AA, Gomis S, Mirakhur K, Li Y *et al*. Analysis of the contribution of *Salmonella* pathogenicity islands 1 and 2 to enteric disease progression using a novel bovine ileal loop model and a murine model of infectious enterocolitis. Infect Immun. 2005;73(11):7161-9.

68. Gusterson B, Cowley G, Smith JA, Ozanne B. Cellular localisation of human epidermal growth factor receptor. Cell Biol Int Rep. 1984;8(8):649-58.

69. Kawakami-Kimura N, Narita T, Ohmori K, Yoneda T, Matsumoto K, Nakamura T *et al*. Involvement of hepatocyte growth factor in increased integrin expression on HepG2 cells triggered by adhesion to endothelial cells. Br J Cancer. 1997;75(1):47-53.

70. Heffernan EJ, Wu L, Louie J, Okamoto S, Fierer J, Guiney DG. Specificity of the complement resistance and cell association phenotypes encoded by the outer membrane protein genes rck from Salmonella typhimurium and ail from Yersinia enterocolitica. Infection and immunity. 1994;62(11):5183-6.

824 71. Alikhan NF, Zhou Z, Sergeant MJ, Achtman M. A genomic overview of the population structure
825 of *Salmonella*. PLoS Genet. 2018;14(4):e1007261.
826 72. Yoshida CE, Kruczkiewicz P, Laing CR, Lingohr EJ, Gannon VP, Nash JH *et al*. The *Salmonella In*
827 *Silico* Typing Resource (SISTR): An Open Web-accessible tool for rapidly typing and subtyping
828 draft *Salmonella* genome assemblies. PLoS One. 2016;11(1):e0147101.
829 73. Nei M. Molecular Evolutionary Genetics. Columbia University Presss. 1987;New-York.
830 74. Paradis E. pegas: an R package for population genetics with an integrated-modular approach.
831 Bioinformatics. 2010;26(3):419-20.
832 75. Esko JD, Stewart TE, Taylor WH. Animal cell mutants defective in glycosaminoglycan
833 biosynthesis. Proc Natl Acad Sci USA. 1985;82(10):3197-201.
834 76. Simon R, Priefer U, Pühler A. A broad host range mobilization system for *in vivo* genetic
835 engineering: transposon mutagenesis in Gram negative bacteria. Bio/Technology. 1983;1:784-
836 91.
837 77. Overton WR. Modified histogram subtraction technique for analysis of flow cytometry data.
838 Cytometry. 1988;9(6):619-26.
839 78. Burlaud-Gaillard J, Sellin C, Georgeault S, Uzbekov R, Lebos C, Guillaume JM *et al*. Correlative
840 scanning-transmission electron microscopy reveals that a chimeric flavivirus is released as
841 individual particles in secretory vesicles. PLoS One. 2014;9(3):e93573.
842 79. Casadaban MJ, Cohen SN. Analysis of gene control signals by DNA fusion and cloning in
843 *Escherichia coli*. J Mol Biol. 1980;138(2):179-207.

844

845 **Figures Legends**

846 **Figure 1: Distribution of allelic variants of *pagN* within *Salmonella* genus.** (**A**) The
847 distribution of *pagN* allelic variants was determined within subspecies *enterica*, *salamae*,
848 *arizonae*, *diarizonae*, *houtenae*, *indica* and species *bongori.* Richness (R) and haplotype
849 diversity (Hd) was measured to evaluate polymorphism. Each colour represents an allelic

variant. n represents the number of genomes for each species/subspecies. (**B**) Distribution of *pagN* allelic variants within 17 out of the 20 most isolated serovars in Europe in 2017. n corresponds to the number of genomes for each serovar. We considered the alleles found in >1% of the strains in a given serovar. Each allele was designated by the number used in Enterobase. Each colour represents an allelic variant, except black which corresponds to the variants showing frequencies under 0.01 for these serovars. Except for the allelic variants showing frequencies under 0.01, the identity percentages were calculated using the protein encoded by allele designated as No. 1 set as reference.

Figure 2: PagN is able to induce both adhesion and invasion depending on the cell line. CHO cells were infected with *HB101-psup* (hatched bars) or *HB101-pagN* strain (empty bars) at 37 °C for 1 h (MOI 1:10). The percentages of total cell-associated (**A**) and internalized (**B**) bacteria have been calculated as described in Materials and Methods. Data show mean values ± SD acquired from three independent experiments with two infected wells per experiment. Data were compared using a Mann Whitney test (***$p<0.001$, **$p<0.01$).

Figure 3: The presence of heparan sulfate is not correlated to the level of PagN-mediated internalization. (**A**) The distribution of HS was analyzed on the cell surface of CHO, pgsA745, Caco-2 and HT29 cell lines by flow cytometry using a specific anti-HS antibody. The percentage of HS positive (HS+) cells was calculated using histogram subtraction (method of Overton) for each cell line as described in the Materials and Methods. (**B**) CHO, pgsA745 and Caco-2 cells were infected with *HB101-pagN* strain at 37 °C for 1 h (MOI 1:10). The percentage of internalized bacteria was calculated as described in Materials and Methods and related to values obtained for CHO cells, set at 100 %. Results represent mean values ± SD obtained from

three independent experiments. Results were compared using a Mann Whitney test (***p<0.001, **p<0.01).

Figure 4. The binding and invasiveness of *Yersinia* Invasin require β1 integrin receptor. F9, triple knockout (TKO) and double knockout (DKO) cells were infected with *MC-InvGFP* strain at MOI 1:10 at 37°C for 1 h. The percentage of total cell-associated (**A**) and intracellular (**B**) bacteria was determined as described in Materials and Methods. Obtained results are expressed relative to values obtained with F9 cells, set at 100 %. Results were compared using a Mann Whitney test (***p<0.001, **p<0.01)

Figure 5: HSPG and β1 integrin cooperate to induce PagN-mediated internalization. (A-B) Parental F9, triple knockout (TKO) and double knockout (DKO) cells were infected with *HB101-pagN* at MOI 1:10 at 37°C for 1 h. (**A**) Percentages of total cell-associated bacteria and (**B**) internalized bacteria were determined as described in the Materials and Methods. Results shown are expressed relative to values got with the parental F9 cells (F9), set at 100 %. (**C-D**) pgsA745 cells were untreated or treated with integrin β1 blocking and IgG at 50 µg/mL for 30 min at 4 °C prior to the addition of *HB101-pagN* or *HB101-psup* at MOI 1:10 for 1 h at 37 °C. (**C**) Percentages of total cell-associated bacteria and (**D**) internalized bacteria were determined as described in the Materials and Methods. Results obtained are expressed relative to values obtained for untreated cells infected with *HB101-pagN*, arbitrarily set at 100%. Results represent means ± SD of three independent experiments with two infected wells per experiment. Results were compared using a Mann Whitney test (****p<0.0001, **p<0.01).

Figure 6: PagN and Rck of *S.* Typhimurium are able to bind to and induce bacterial invasion, leading to a local remodeling of the host actin cytoskeleton. (**A**) CHO and Jeg-3

cells were incubated with either PagN- or Rck-coated beads, respectively. After 30 min of contact between cells and coated beads at 37 °C, cells were washed and then stained by immunofluorescence. Horizontal sections of cells obtained with confocal laser scanning microscopy shows actin staining in red and overlay of beads in green and actin; Representative images are shown with an arrow, indicating the site of actin polymerization and typical structural morphologies. (**B**-**C**) Jeg-3 cells were infected with *MC1061 psup* or *MC1061-rck* strain for 1 h at 37 °C (MOI 1:10). The percentages of total cell-associated (**B**) and internalized (**C**) bacteria were determined as described in the Materials and Methods. Results are mean values ± SD acquired with three independent experiments with two infected wells per experiment. Results were compared using a Mann Whitney test (**p<0.01).

Figure 7: Rck and PagN of *S.* Typhimurium mediate a Zipper-like entry mechanism. (**A-B**) CHO cells were incubated with PagN-beads (**A**) or *HB101-pagN* (**B**). (**C-D**) Jeg-3 cells were incubated with Rck-beads (**C**) or *MC1061-rck* (**D**). After 1 h, the cells were washed and then processed for scanning electron microscopy.

Figure 8: Class I PI 3-kinase p85α-p110 is required for Rck- and PagN-mediated internalization. CHO (**A-B**) or Jeg-3 (**C-D**) cells were incubated with AS604850 at the indicated concentrations for 2 h 30 prior to the addition of *HB101-pagN* (**A-B**) or *MC1061-rck* (**C-D**) at MOI 1:10 for 1 h at 37 °C. Percentages of total cell-associated bacteria (**A-C:** grey bars) and internalized bacteria (**B-D:** white bars) were determined as described in the Materials and Methods. Results acquired with drugs are expressed relative to values acquired for the same amount of DMSO-containing medium (DMSO), set at 100 %.CHO (**E-F**) and Jeg-3 (**G-H**) cells transfected with Δp85α and Wp85α were infected with *HB101-pagN* (**E-F**) or *MC1061-rck* (**G-H**) at MOI 1:10 at 37 °C for 1 h. The percentages of total cell-associated bacteria (**E-G:** grey

bars) and internalized bacteria (**F-H:** white bars) were calculated and expressed relative to values obtained for Wp85 α transfected cells, set at 100%. Values represent means ± SD of three independent experiments with two infected wells per experiment. Results were compared using a Mann Whitney test (***p<0.001, **p<0.01).

Figure 9: Protein tyrosine kinases are required for Rck- and PagN-mediated internalization. CHO (**A-B**) or Jeg-3 (**C-D**) cells were incubated with genistein at the indicated concentrations for 15min prior to the addition of *HB101-pagN (***A-B***)* or *MC1061-rck* (**C-D**) at MOI 1:10 for 1 h at 37°C. Percentages of total cell-associated bacteria (**A-C:** grey bars) and internalized bacteria (**B-D:** white bars) were determined as described in the Materials and Methods. Results obtained with drugs are expressed relative to values obtained for the same amount of DMSO-containing medium (DMSO), arbitrarily set at 100 %. Data were compared using a Mann Whitney test **p<0.01, *p<0.05).

938 **TABLE 1: Abilities of latex beads coated with different GST fusion proteins to bind and mediate**

939 **actin recruitment and internalization**

940

Coated beads	Adhesion	Actin recruitment	Internalization
GST	---	---	---
GST-113-159Rck	+++	+++	+++
GST-PagN	+++	+++	+++

941 (-): non-detectable; (+) low, (++) medium and (+++) high level

942 **TABLE 2: Bacterial strains and plasmids used in this study**

943 Cb^r, carbenicillin resistance; Tc^r, tetracyclin resistance; Cm^r, chloramphenicol resistance.

944

Strain or plasmid	Relevant characteristic(s)	Source or reference
Strains		
HB101	Noninvasive laboratory strain (s*upE44 hsdS20*($r_B^- m_B^-$) *recA13 ara-14 proA2 lacY1 galK2 rpsL20 xyl-5 mtl-1 leuB6 thi-1*)	Promega
BL21 pLysS	An *E. coli* strain which is lysogenic for λ-DE3 and contains the T7 bacteriophage gene I, encoding T7 RNA polymerase under the control of the *lac* UV5 promoter as well as a plasmid, pLysS, which carries the gene encoding T7 lysozyme (Cm^r)	Promega
MC1061	*E. coli* hsdR mcrB araD139 Δ(araABC-leu)7679 ΔlacX74 galU galK rpsL thi	[79]
Plasmids		
pSUP202	pMB1 replicon (Cb^r, Tc^r, Cm^r)	[76]
pSUP202-Rck	Vector carrying the *rck* gene (Cb^r, Cm^r)	[14]
pSUP202-PagN	Vector carrying the *pagN* gene (Cb^r, Cm^r)	This study
pSUP2020-Inv GFP	Vector carrying the *invasin* gene from *Yersinia enterocolitica* and *gfp* gene (Cb^r)	[14]
pGEX-4T-2	Fusion vector carrying the glutathione S-transferase gene (Cb^r)	GE Healthcare
pGEX-4T-2 114-159 Rck	Vector carrying the glutathione S-transferase (GST) gene linked to 113-159 *rck* gene (Cb^r)	[10]
pGEX-4T-2 PagN	Vector carrying the glutathione S-transferase (GST) gene linked to *pagN* gene (Cb^r)	This study
pcDNA 3.1 Wp85	Vector carrying the wild-type bovine *p85α* sequence (Cb^r)	[12]
pcDNA 3.1 Δp85	Vector carrying the mutant bovine *p85α* sequence (Cb^r)	[12]

945 **TABLE 3: Primers used in this study**

946

Primer name	Sequence (5′ to 3′)
pagN EcoRI forw	CTC GAA TTC ATT AAG GCA GGT TCT GAA ATG
pagN NcoI rev	TCT CCA TGG TTA AAA GGC GTA AGT AAT GCC
pagN-GST forw	CTC GGA TCC CAT CAT CAT CAT CAT CAT AAA GAA GGG ATC TAT ATC ACC GGG A
pagN-GST rev	TCT GAA TTC TTA AAA GGC GTA AGT AAT GCC GAG
Forw pcDNA3.1	GAC TCA CTA TAG GGA GAC CCA AGC TGG CTA
Rev pcDNA3.1	GCT GGG CAA CTA GAA GGC ACA GTC GAG GCT

947

Figure 1

A

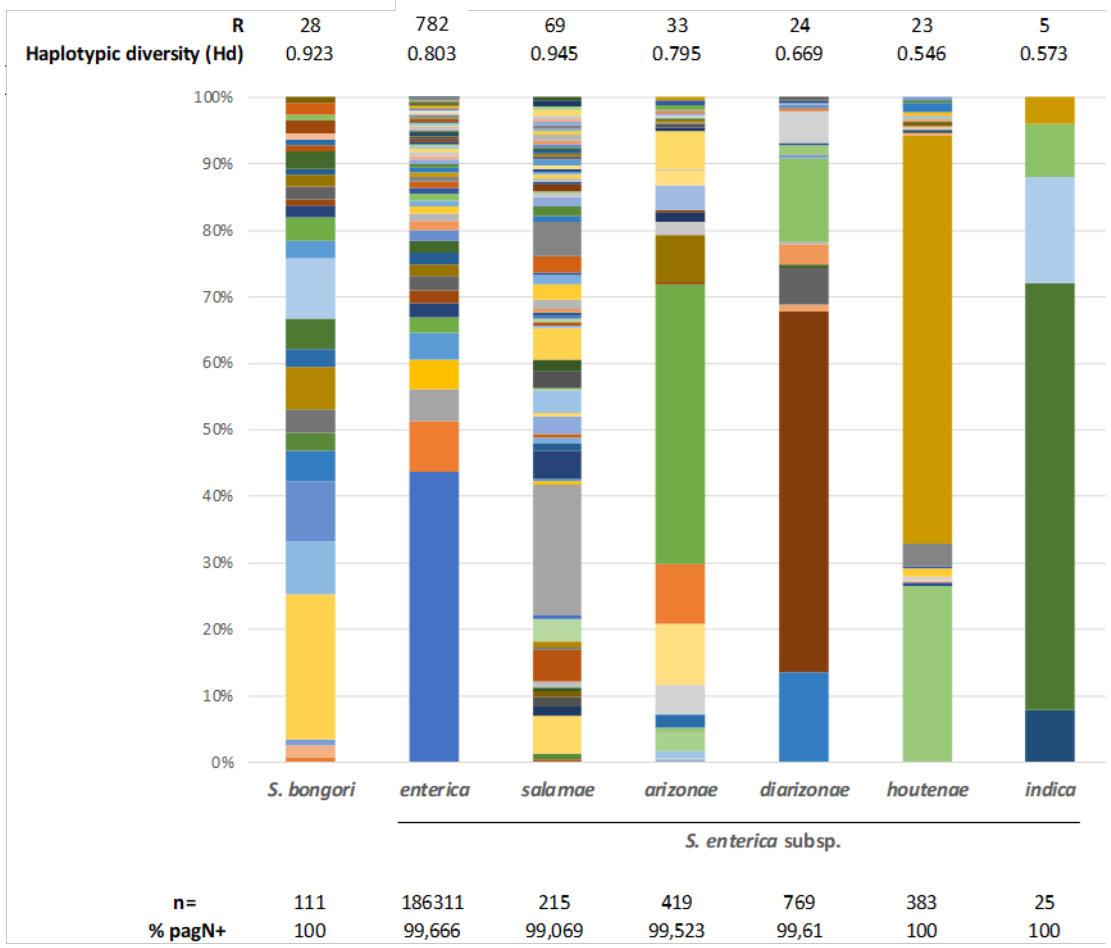
R 28 782 69 33 24 23 5
Haplotypic diversity (Hd) 0.923 0.803 0.945 0.795 0.669 0.546 0.573
100%
90%
80%
70%
60%
50%
40%
30%
20%
10%
0%
S. bongori
enterica
salamae
arizonae
diarizonae
houtenae
indica
S. enterica subsp.
n= 111 186311 215 419 769 383 25
% pagN+ 100 99,666 99,069 99,523 99,61 100 100

B

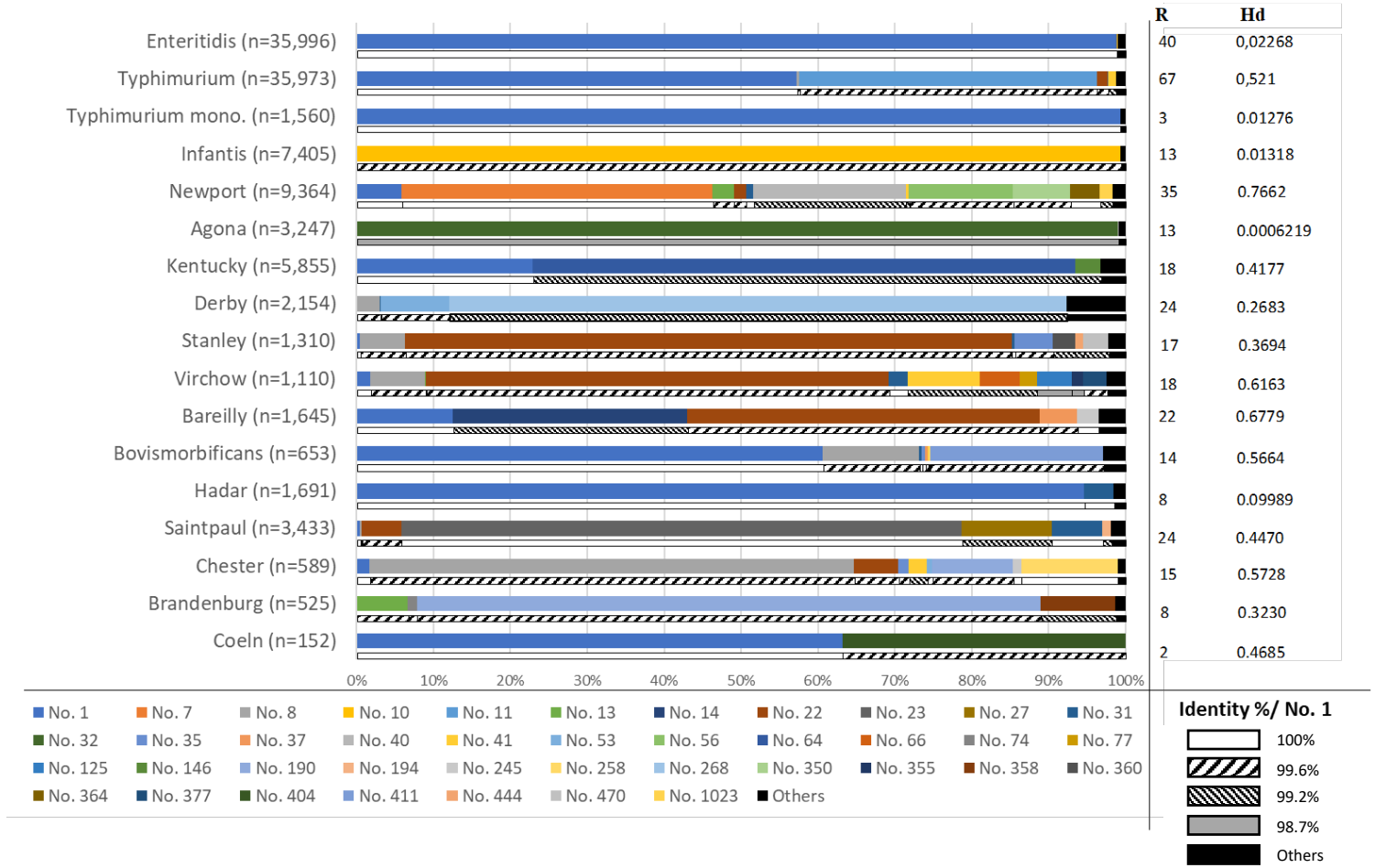
Enteritidis (n=35,996)
Typhimurium (n=35,973)
Typhimurium mono. (n=1,560)
Infantis (n=7,405)
Newport (n=9,364)
Agona (n=3,247)
Kentucky (n=5,855)
Derby (n=2,154)
Stanley (n=1,310)
Virchow (n=1,110)
Bareilly (n=1,645)
Bovismorbificans (n=653)
Hadar (n=1,691)
Saintpaul (n=3,433)
Chester (n=589)
Brandenburg (n=525)
Coeln (n=152)
R
Hd
40 0,02268
67 0,521
3 0.01276
13 0.01318
35 0.7662
13 0.0006219
18 0.4177
24 0.2683
17 0.3694
18 0.6163
22 0.6779
14 0.5664
8 0.09989
24 0.4470
15 0.5728
8 0.3230
2 0.4685
0% 10% 20% 30% 40% 50% 60% 70% 80% 90% 100%
No. 1 No. 7 No. 8 No. 10 No. 11 No. 13 No. 14 No. 22 No. 23 No. 27 No. 31
No. 32 No. 35 No. 37 No. 40 No. 41 No. 53 No. 56 No. 64 No. 66 No. 74 No. 77
No. 125 No. 146 No. 190 No. 194 No. 245 No. 258 No. 268 No. 350 No. 355 No. 358 No. 360
No. 364 No. 377 No. 404 No. 411 No. 444 No. 470 No. 1023 Others
Identity %/ No. 1
100%
99.6%
99.2%
98.7%
Others

Figure 2

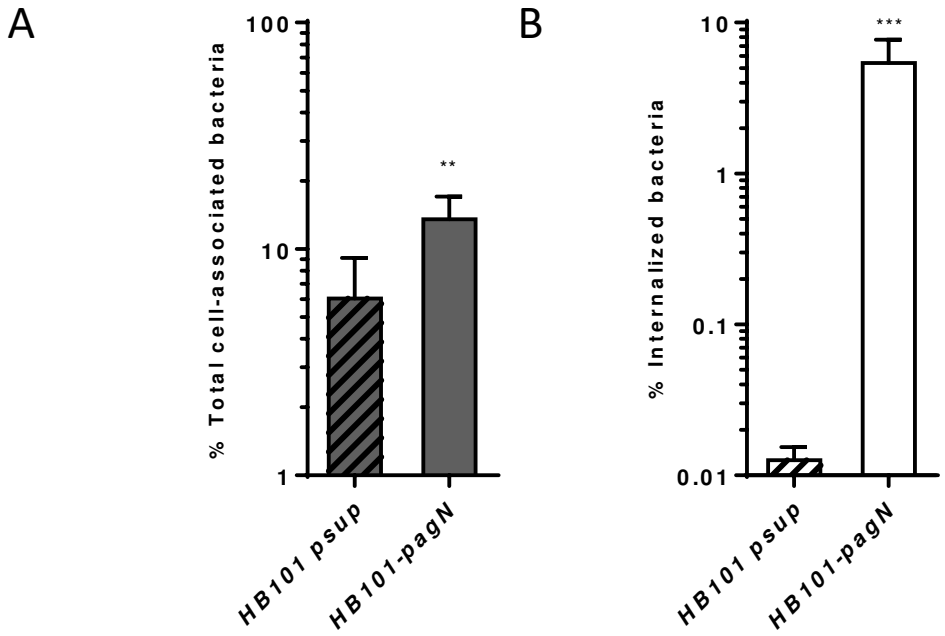
A
100
10
1
% Total cell-associated bacteria
**
HB101 psup
HB101-pagN
B
10
1
0.1
0.01
% Internalized bacteria
***
HB101 psup
HB101-pagN

Figure 3

A

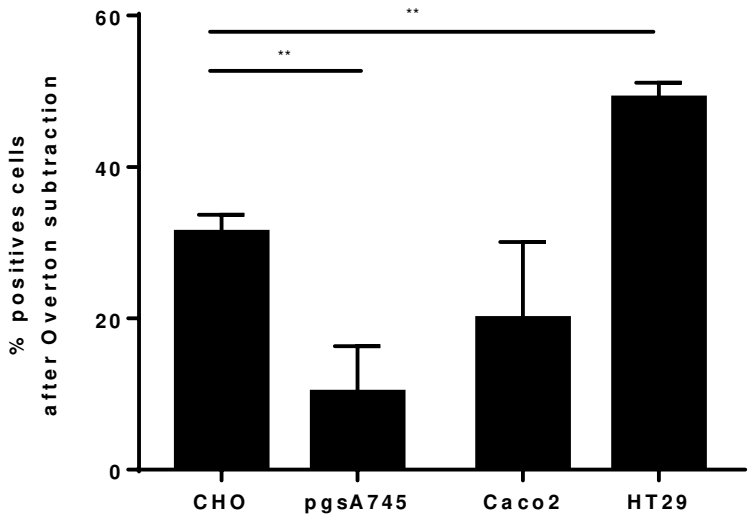
% positives cells
after Overton subtraction
60
40
20
0
**
**
CHO
pgsA745
Caco2
HT29

B

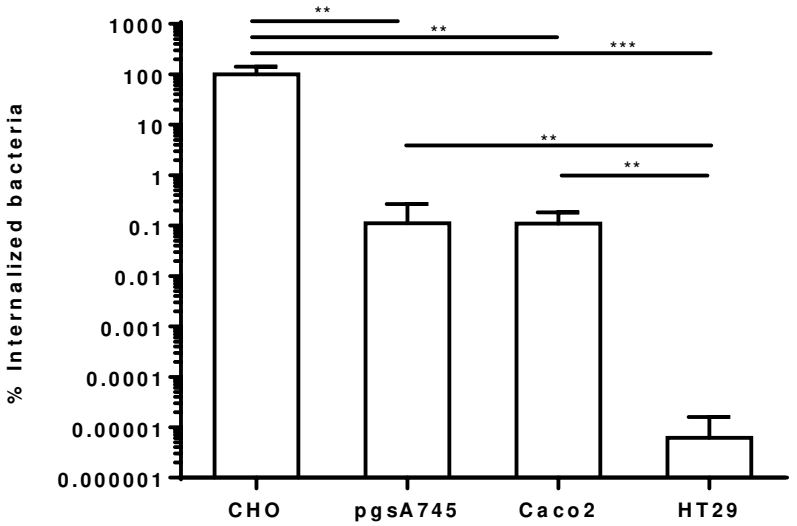
% Internalized bacteria
1000
100
10
1
0.1
0.01
0.001
0.0001
0.00001
0.000001
**
**
***
**
**
CHO
pgsA745
Caco2
HT29

Figure 4

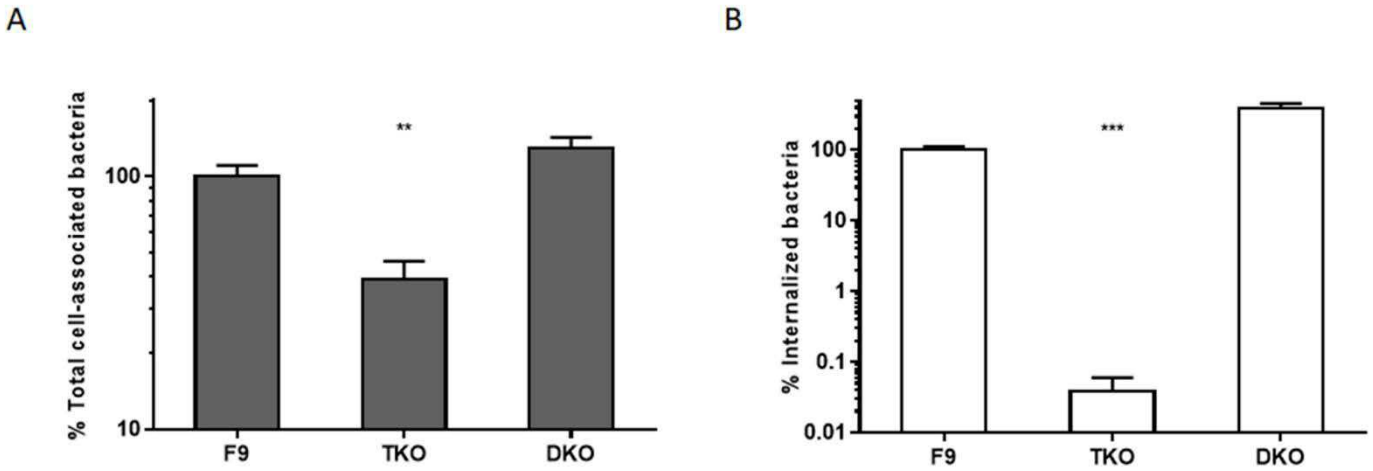
A
% Total cell-associated bacteria
100
10
**
F9
TKO
DKO
B
% Internalized bacteria
100
10
1
0.1
0.01
***
F9
TKO
DKO

Figure 5

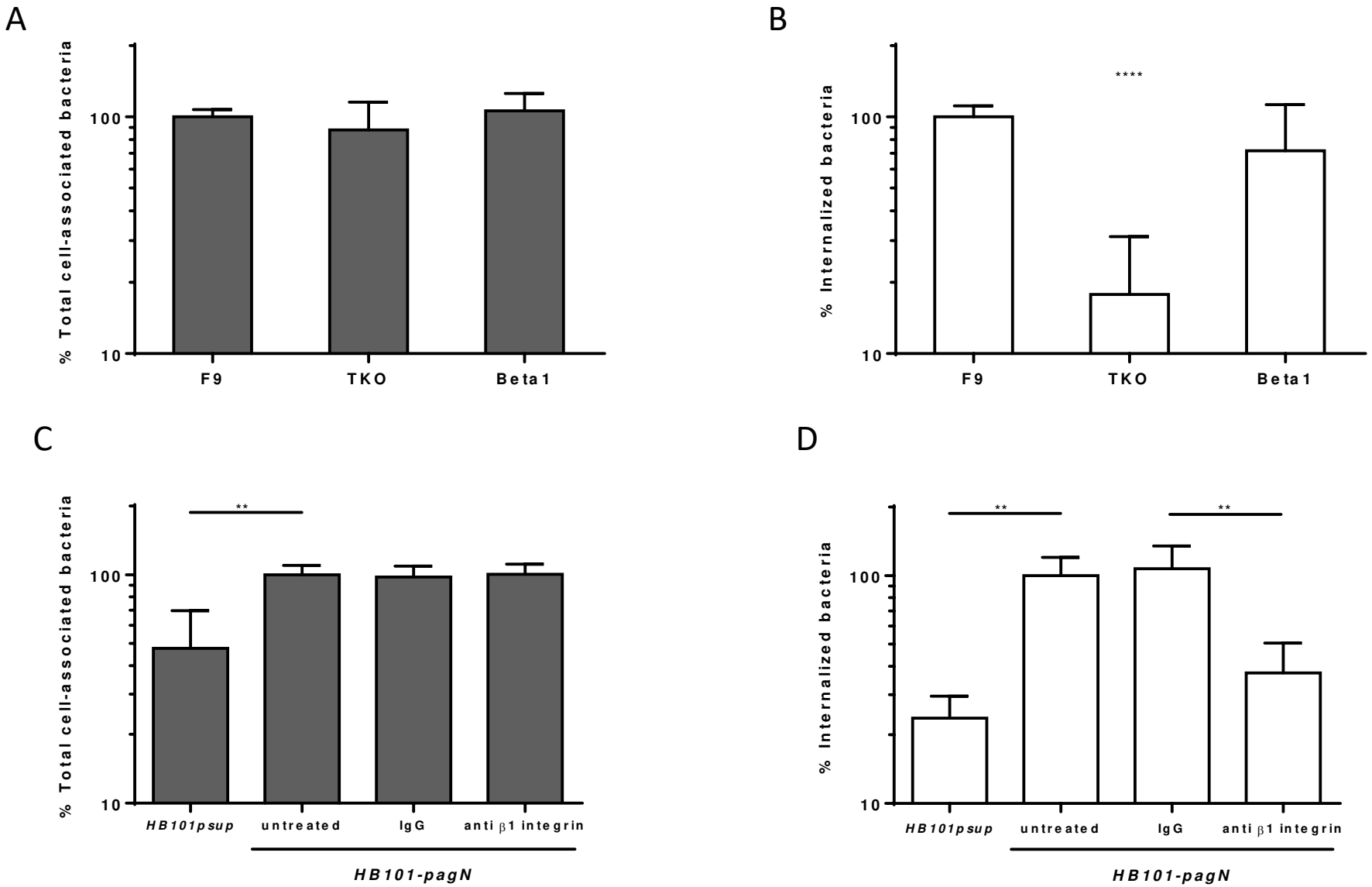
A
% Total cell-associated bacteria
100
10
F9
TKO
Beta1
B
% Internalized bacteria
****
100
10
F9
TKO
Beta1
C
% Total cell-associated bacteria
**
100
10
HB101psup
untreated
IgG
anti β1 integrin
HB101-pagN
D
% Internalized bacteria
**
**
100
10
HB101psup
untreated
IgG
anti β1 integrin
HB101-pagN

Figure 6

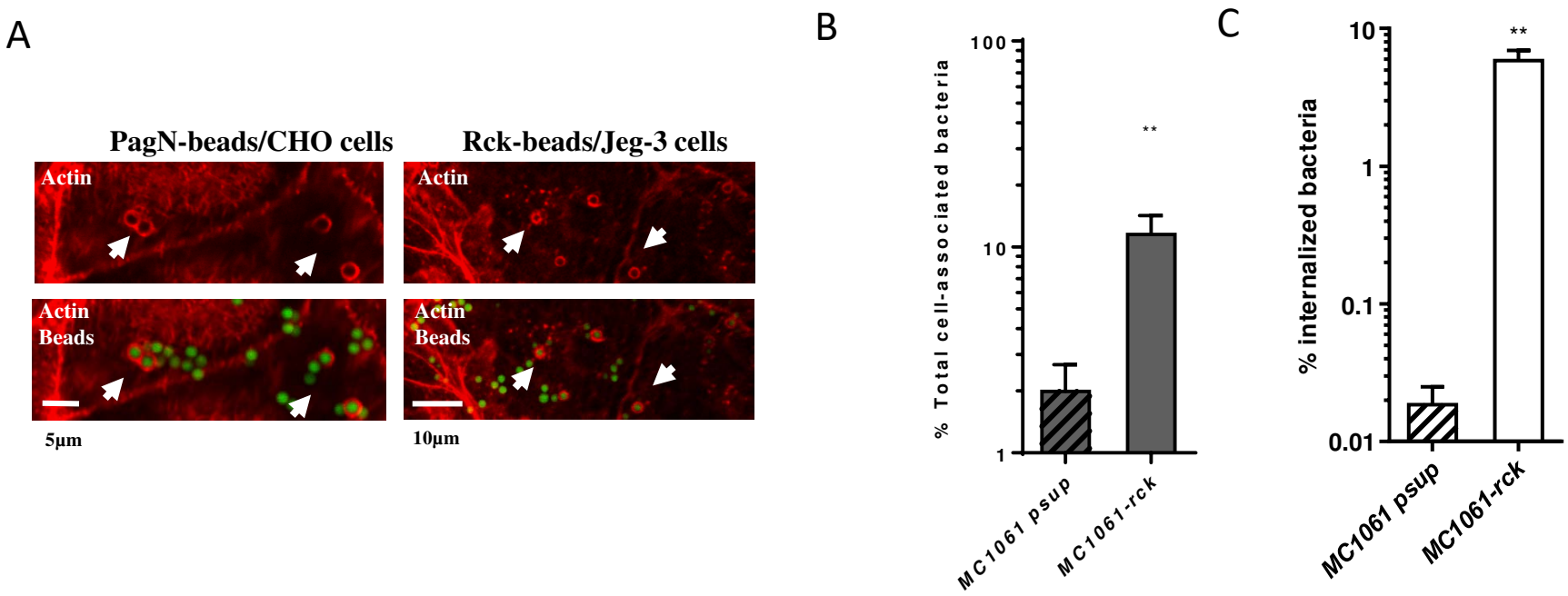
A
PagN-beads/CHO cells
Rck-beads/Jeg-3 cells
Actin
Actin
Actin
Beads
Actin
Beads
5µm
10µm
B
% Total cell-associated bacteria
100
10
1
**
MC1061 psup
MC1061-rck
C
% internalized bacteria
10
1
0.1
0.01
**
MC1061 psup
MC1061-rck

Figure 7

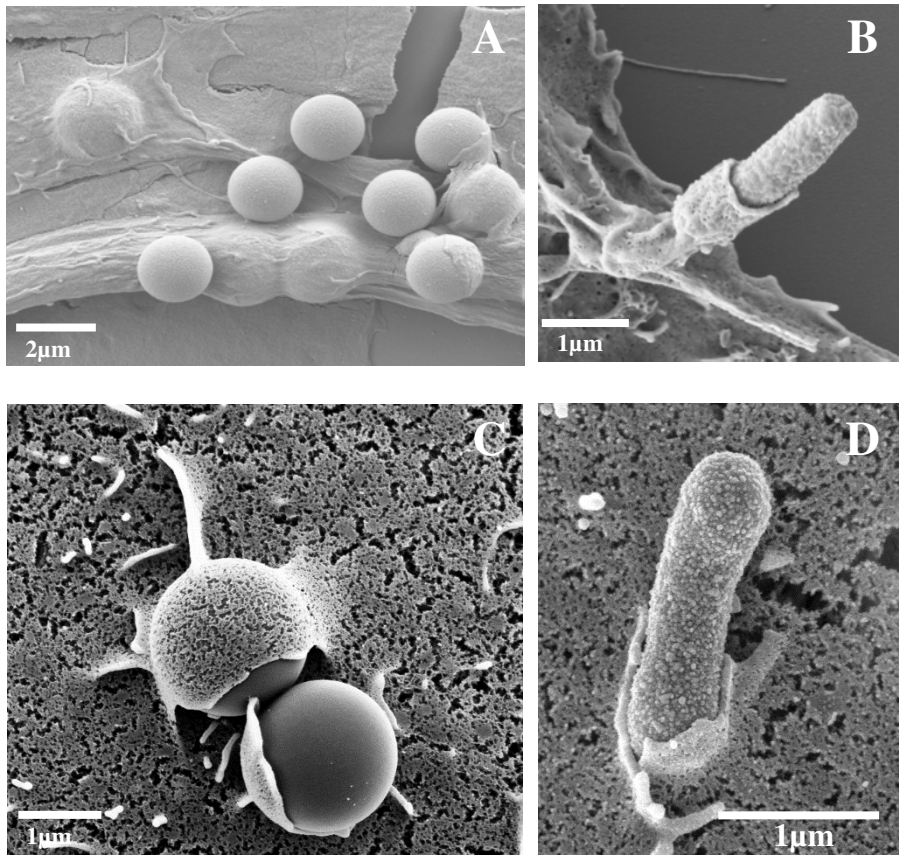

Figure 8

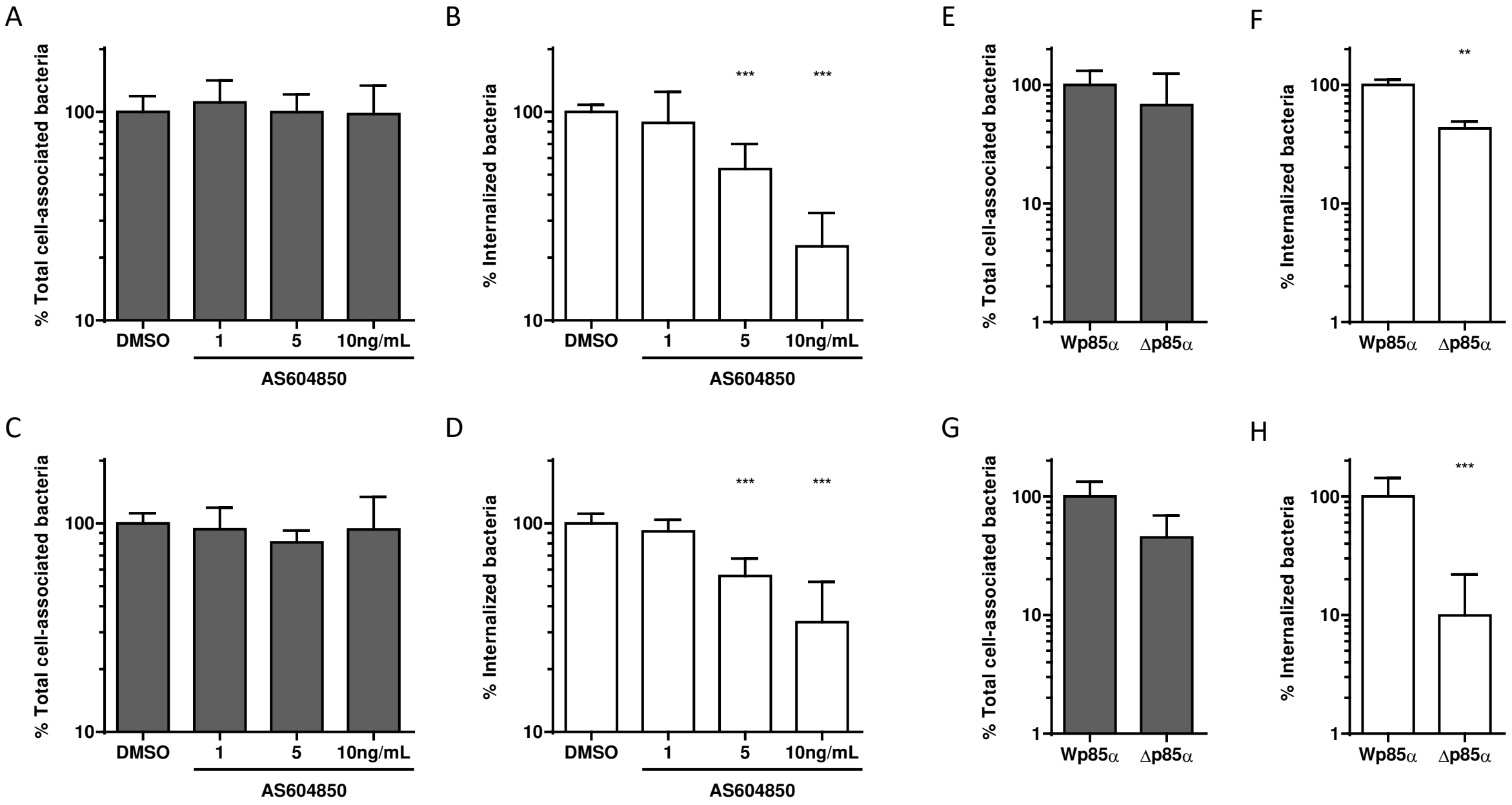
A
B
E
F
C
D
G
H
% Total cell-associated bacteria
% Internalized bacteria
100
10
1
DMSO
1
5
10ng/mL
AS604850
***
**
Wp85α
Δp85α

Figure 9

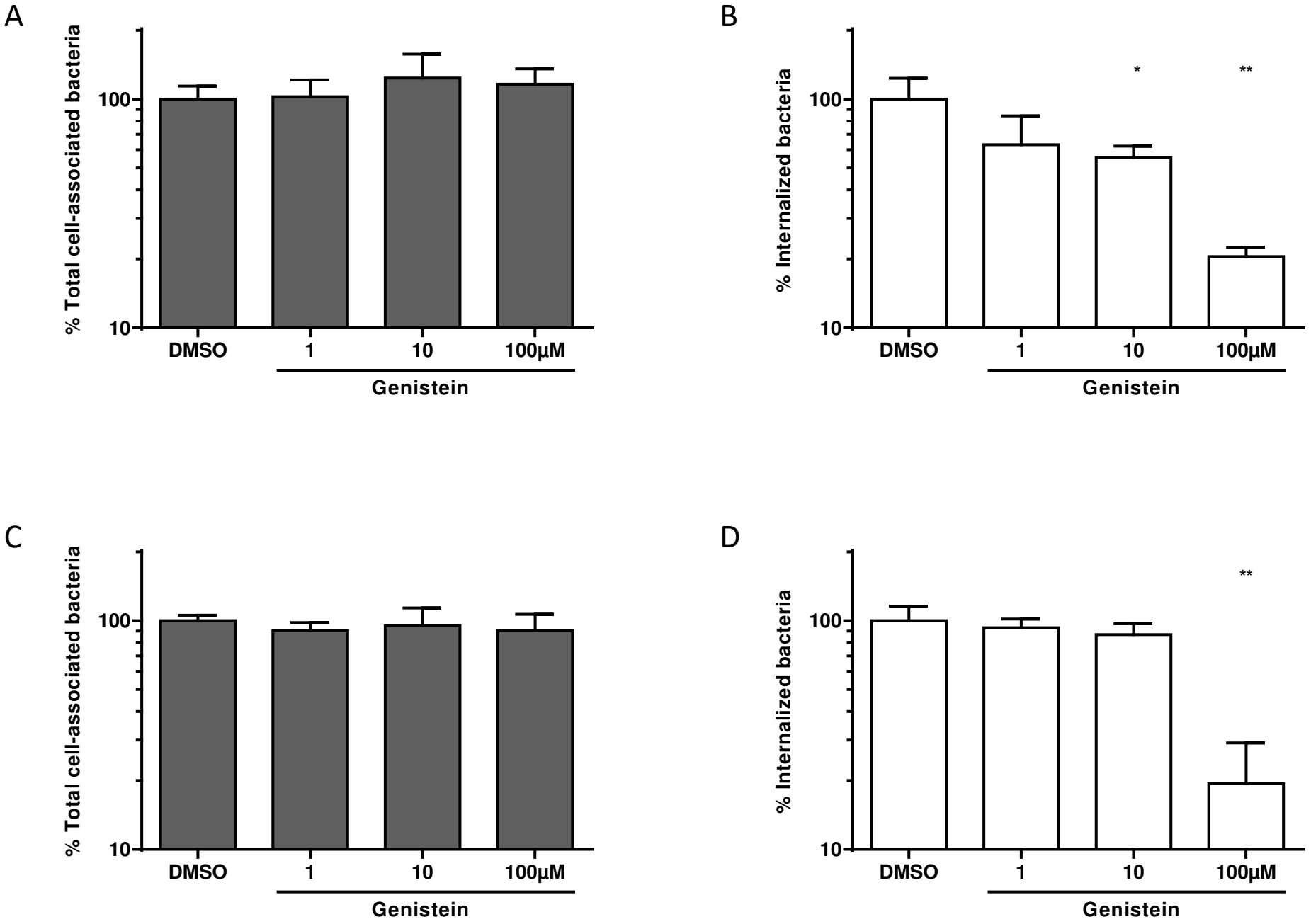
A
% Total cell-associated bacteria
100
10
DMSO
1
10
100µM
Genistein
B
% Internalized bacteria
100
10
*
**
DMSO
1
10
100µM
Genistein
C
% Total cell-associated bacteria
100
10
DMSO
1
10
100µM
Genistein
D
% Internalized bacteria
100
10
**
DMSO
1
10
100µM
Genistein

Figures

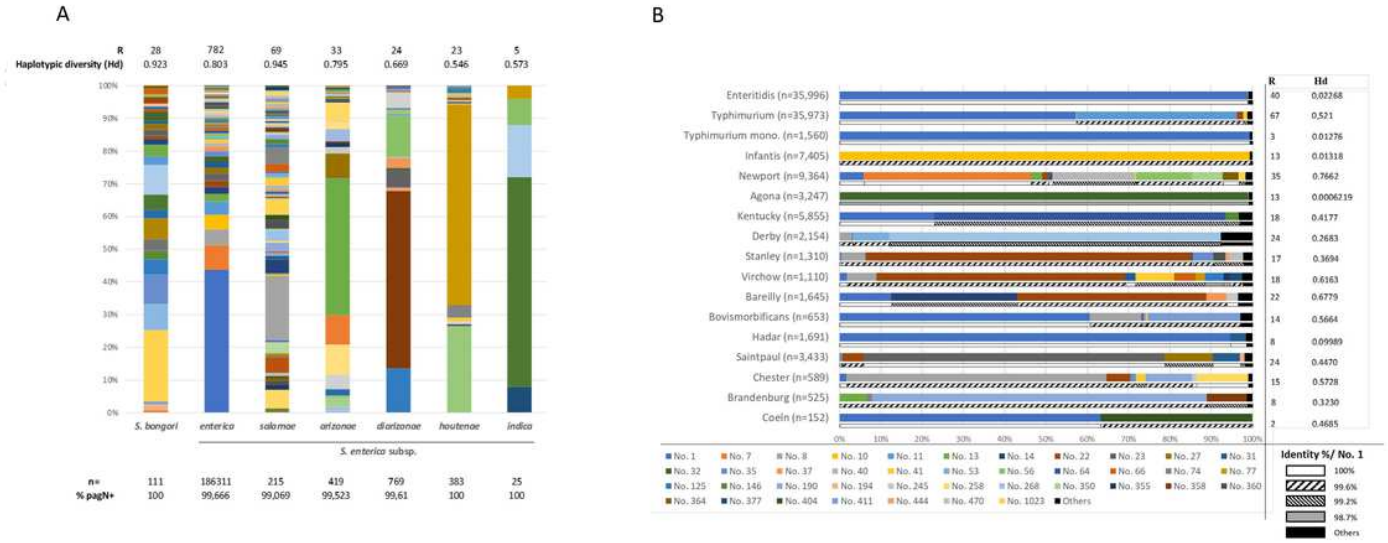

Figure 1

Distribution of allelic variants of pagN within Salmonella genus. (A) The 846 distribution of pagN allelic variants was determined within subspecies enterica, salamae, arizonae, diarizonae, houtenae, indica and species bongori. Richness (R) and haplotype diversity (Hd) was measured to evaluate polymorphism. Each colour represents an allelic variant. n represents the number of genomes for each species/subspecies. (B) Distribution of pagN allelic variants within 17 out of the 20 most isolated serovars in Europe in 2017. n corresponds to the number of genomes for each serovar. We considered the alleles found in >1% of the strains in a given serovar. Each allele was designated by the number used in Enterobase. Each colour represents an allelic variant, except black which corresponds to the variants showing frequencies under 0.01 for these serovars. Except for the allelic variants showing frequencies under 0.01, the identity percentages were calculated using the protein encoded by allele designated as No. 1 set as reference.

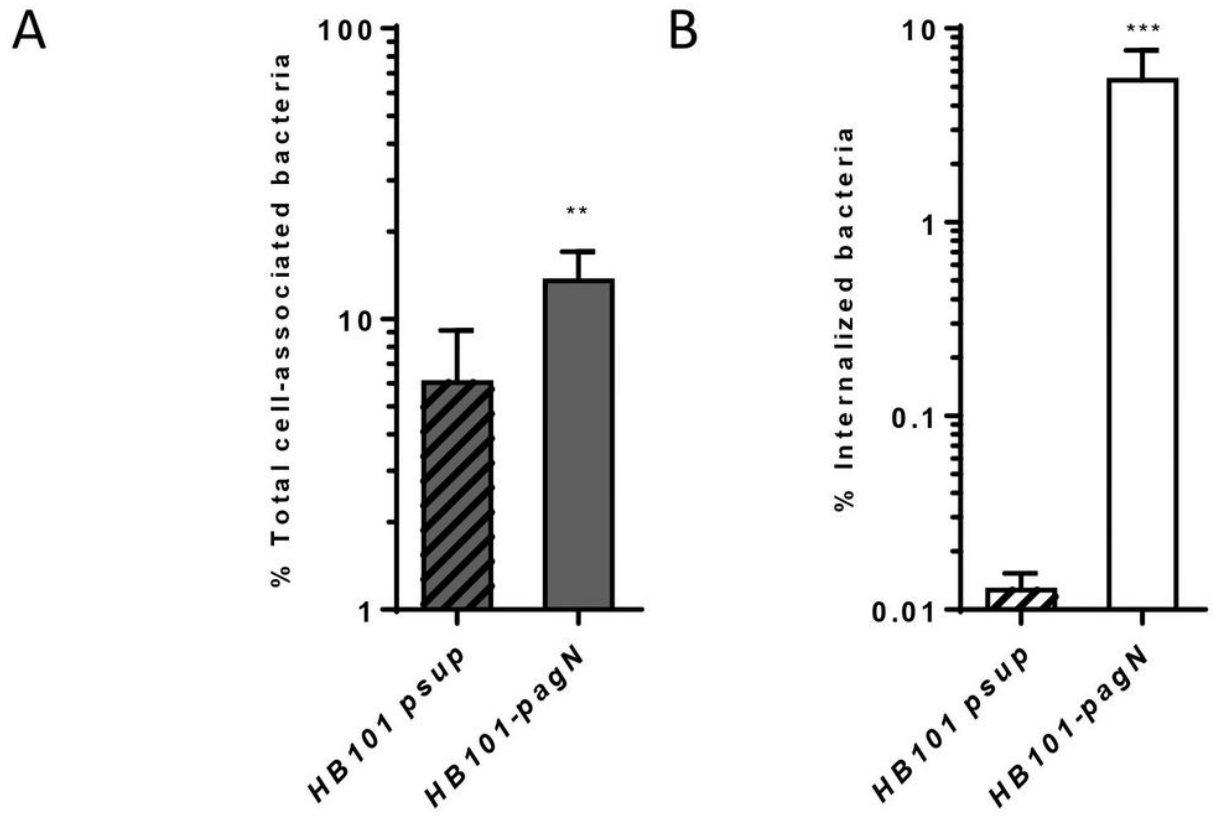

Figure 2

PagN is able to induce both adhesion and invasion depending on the cell line. CHO cells were infected with HB101-psup (hatched bars) or HB101-pagN strain (empty bars) at 37 °C for 1 h (MOI 1:10). The percentages of total cell-associated (A) and internalized (B) bacteria have been calculated as described in Materials and Methods. Data show mean values ± SD acquired from three independent experiments with two infected wells per experiment. Data were compared using a Mann Whitney test (***$p<0.001$, **$p<0.01$).

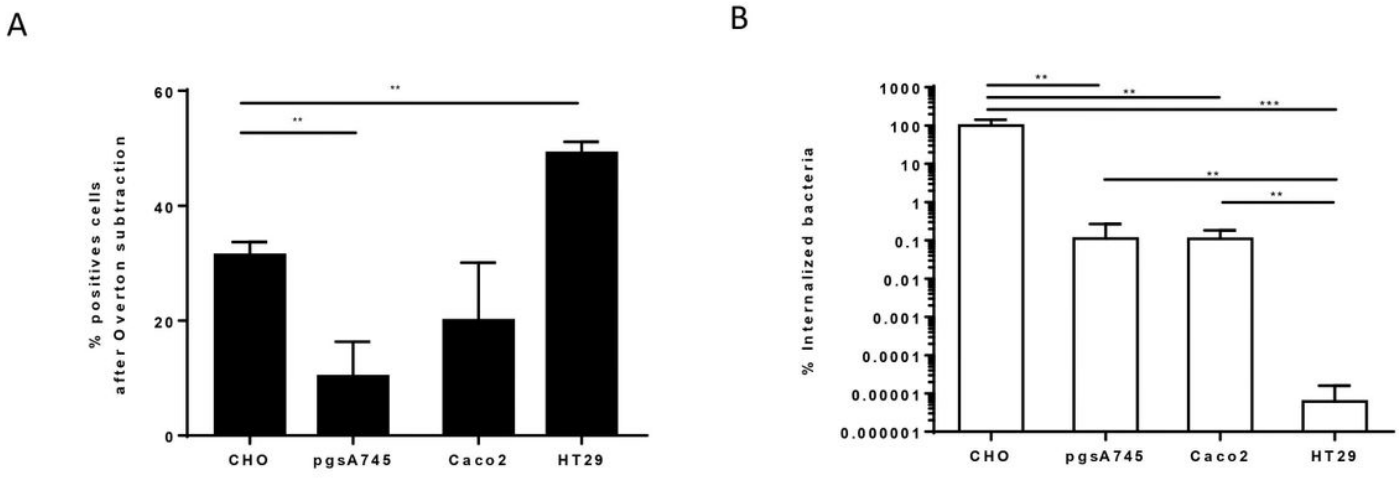

Figure 3

The presence of heparan sulfate is not correlated to the level of PagN-mediated internalization. (A) The distribution of HS was analyzed on the cell surface of CHO, pgsA745, Caco-2 and HT29 cell lines by flow cytometry using a specific anti-HS antibody. The percentage of HS positive (HS+) cells was calculated using histogram subtraction (method of Overton) for each cell line as described in the Materials and Methods. (B) CHO, pgsA745 and Caco-2 cells were infected with HB101-pagN strain at 37 °C for 1 h (MOI 1:10). The percentage of internalized bacteria was calculated as described in Materials and Methods and related to values obtained for CHO cells, set at 100 %. Results represent mean values ± SD obtained from three independent experiments. Results were compared using a Mann Whitney test (***p<0.001, **p<0.01).

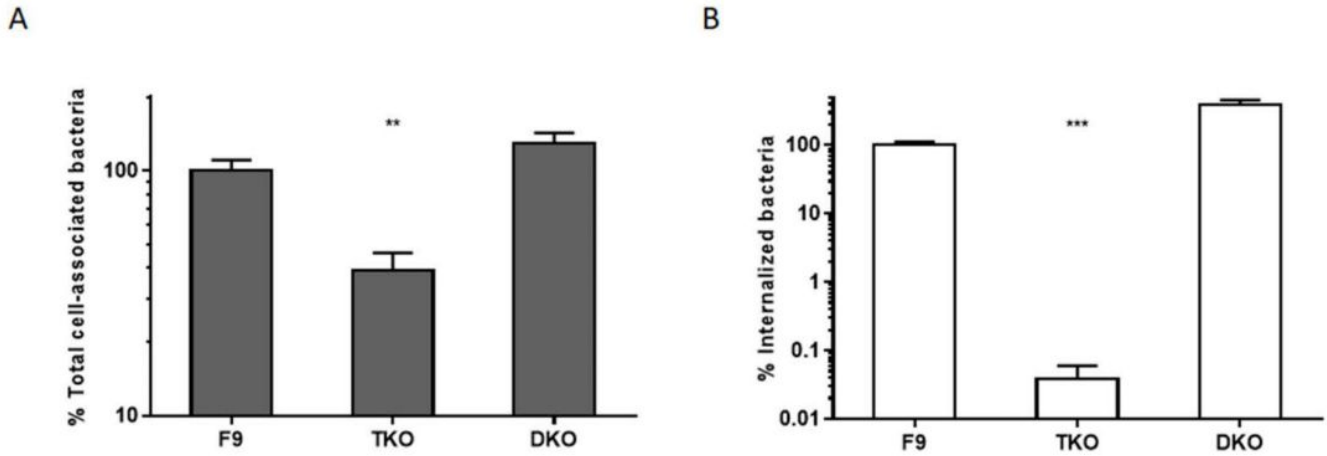

Figure 4

The binding and invasiveness of Yersinia Invasin require β1 integrin receptor. F9, triple knockout (TKO) and double knockout (DKO) cells were infected with MC-InvGFP strain at MOI 1:10 at 37°C for 1 h. The

percentage of total cell-associated (A) and intracellular (B) bacteria was determined as described in Materials and Methods. Obtained results are expressed relative to values obtained with F9 cells, set at 100 %. Results were compared using a Mann Whitney test (***p<0.001, **p<0.01)

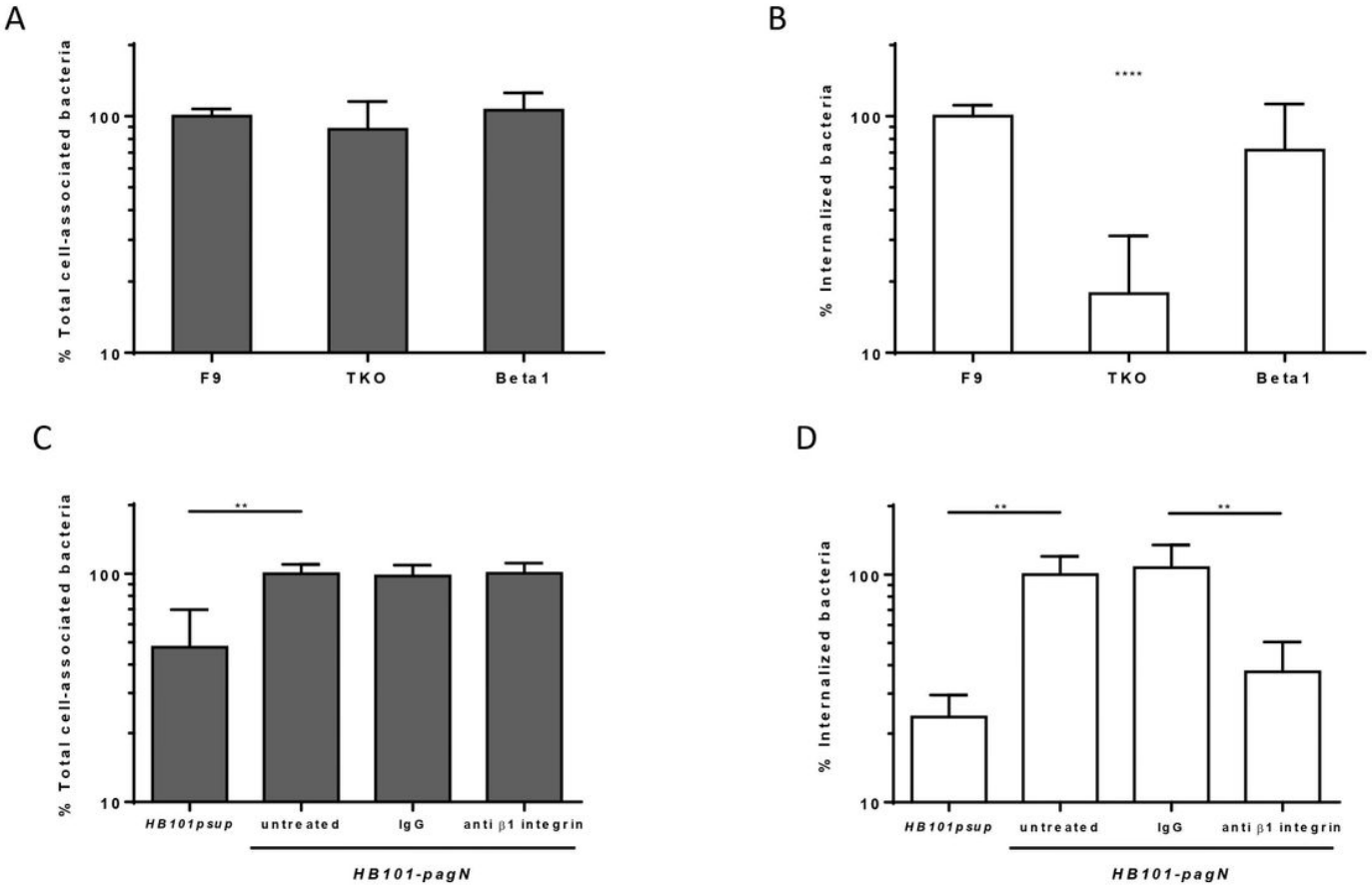

Figure 5

HSPG and β1 integrin cooperate to induce PagN-mediated internalization. (A- B) Parental F9, triple knockout (TKO) and double knockout (DKO) cells were infected with HB101-pagN at MOI 1:10 at 37°C for 1 h. (A) Percentages of total cell-associated bacteria and (B) internalized bacteria were determined as described in the Materials and Methods. Results shown are expressed relative to values got with the parental F9 cells (F9), set at 100 %. (C-D) pgsA745 cells were untreated or treated with integrin β1 blocking and IgG at 50 µg/mL for 30 min at 4 °C prior to the addition of HB101-pagN or HB101-psup at MOI 1:10 for 1 h at 37 °C. (C) Percentages of total cell-associated bacteria and (D) internalized bacteria were determined as described in the Materials and Methods. Results obtained are expressed relative to values obtained for untreated cells infected with HB101-pagN, arbitrarily set at 100%. Results represent means ± SD of three independent experiments with two infected wells per experiment. Results were compared using a Mann Whitney test (****p<0.0001, **p<0.01).

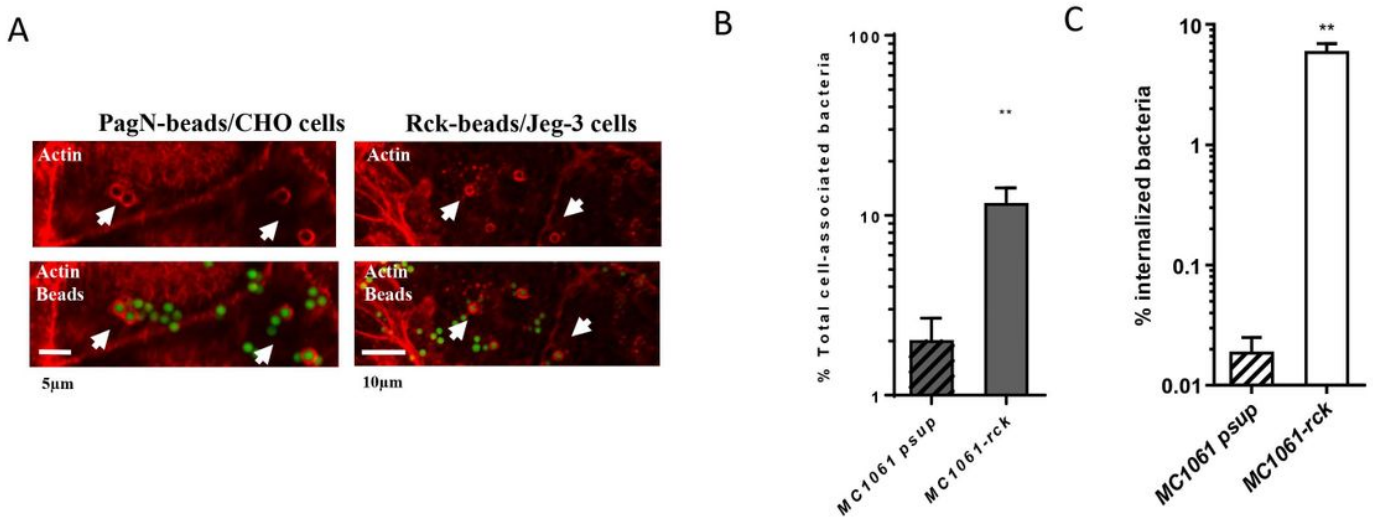

Figure 6

PagN and Rck of S. Typhimurium are able to bind to and induce bacterial 897 invasion, leading to a local remodeling of the host actin cytoskeleton. (A) CHO and Jeg-3 cells were incubated with either PagN- or Rck-coated beads, respectively. After 30 min of contact between cells and coated beads at 37 °C, cells were washed and then stained by immunofluorescence. Horizontal sections of cells obtained with confocal laser scanning microscopy shows actin staining in red and overlay of beads in green and actin; Representative images are shown with an arrow, indicating the site of actin polymerization and typical structural morphologies. (B-C) Jeg-3 cells were infected with MC1061 psup or MC1061-rck strain for 1 h at 37 °C (MOI 1:10). The percentages of total cell-associated (B) and internalized (C) bacteria were determined as described in the Materials and Methods. Results are mean values ± SD acquired with three independent experiments with two infected wells per experiment. Results were compared using a Mann Whitney test (**p<0.01).

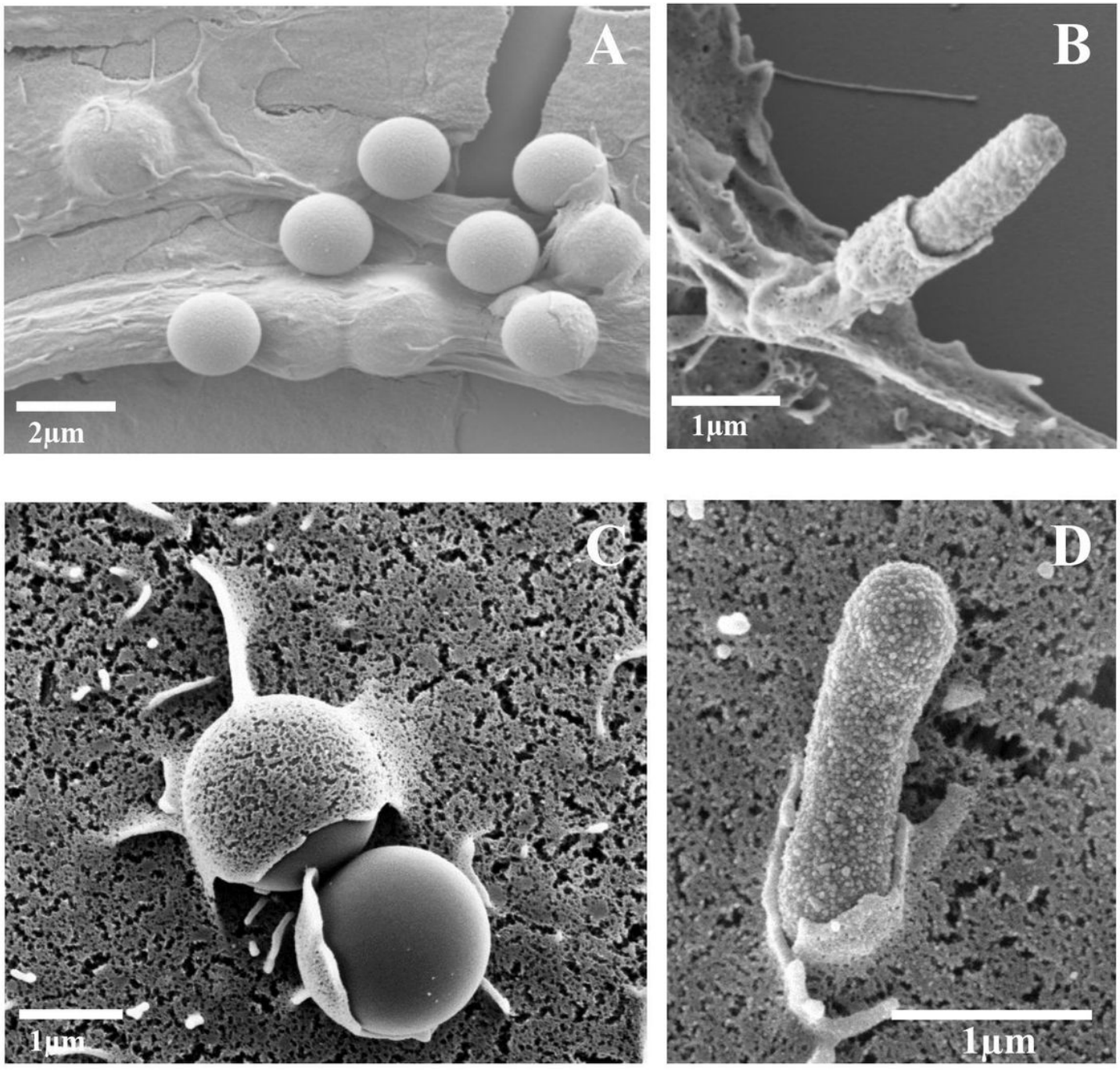

Figure 7

Rck and PagN of S. Typhimurium mediate a Zipper-like entry mechanism. (A- B) CHO cells were incubated with PagN-beads (A) or HB101-pagN (B). (C-D) Jeg-3 cells were incubated with Rck-beads (C) or MC1061-rck (D). After 1 h, the cells were washed and then processed for scanning electron microscopy.

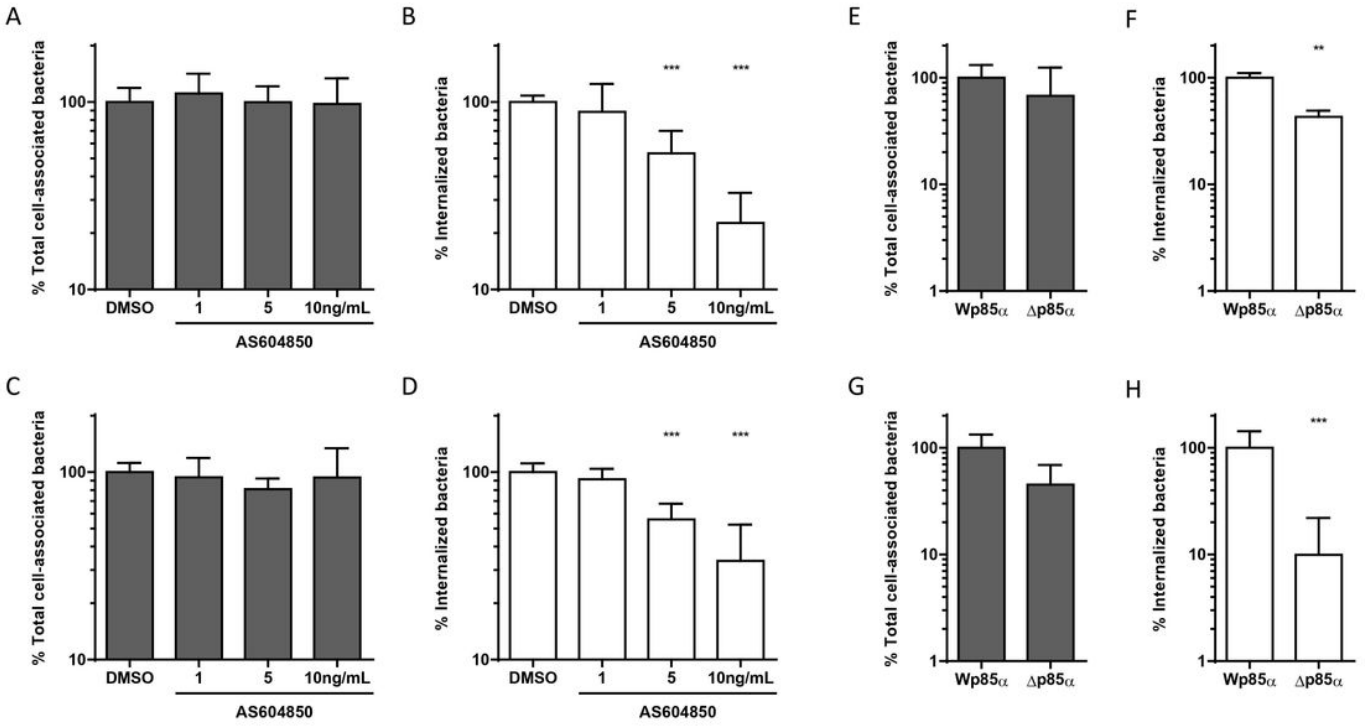

Figure 8

Class I PI 3-kinase p85α-p110 is required for Rck- and PagN-mediated 915 internalization. CHO (A-B) or Jeg-3 (C-D) cells were incubated with AS604850 at the indicated concentrations for 2 h 30 prior to the addition of HB101-pagN (A-B) or MC1061-rck (C-D) at MOI 1:10 for 1 h at 37 °C. Percentages of total cell-associated bacteria (A-C: grey bars) and internalized bacteria (B-D: white bars) were determined as described in the Materials and Methods. Results acquired with drugs are expressed relative to values acquired for the same amount of DMSO-containing medium (DMSO), set at 100 %.CHO (E-F) and Jeg-3 (G-H) cells transfected with Δp85α and Wp85α were infected with HB101-pagN (E-F) or MC1061-rck (G- H) at MOI 1:10 at 37 °C for 1 h. The percentages of total cell-associated bacteria (E-G: grey bars) and internalized bacteria (F-H: white bars) were calculated and expressed relative to values obtained for Wp85 α transfected cells, set at 100%. Values represent means ± SD of three independent experiments with two infected wells per experiment. Results were compared using a Mann Whitney test (***p<0.001, **p<0.01).

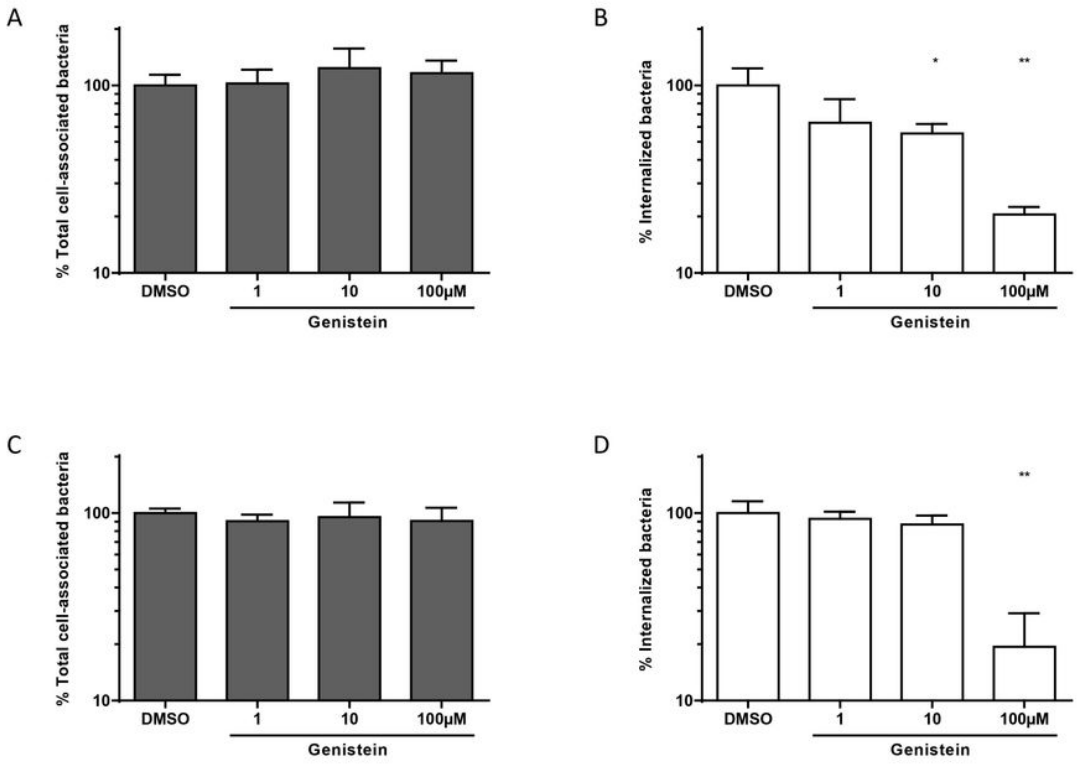

Figure 9

Protein tyrosine kinases are required for Rck- and PagN-mediated 929 internalization. CHO (A-B) or Jeg-3 (C-D) cells were incubated with genistein at the indicated concentrations for 15min prior to the addition of HB101-pagN (A-B) or MC1061-rck (C-D) at MOI 1:10 for 1 h at 37°C. Percentages of total cell-associated bacteria (A-C: grey bars) and internalized bacteria (B-D: white bars) were determined as described in the Materials and Methods. Results obtained with drugs are expressed relative to values obtained for the same amount of DMSO-containing medium (DMSO), arbitrarily set at 100 %. Data were compared using a Mann Whitney test **p<0.01, *p<0.05).